DEVELOPMENT OF THE EVOLVED COMMON HARDWARE BUS (TECHBUS)

A Thesis
Presented to
The Academic Faculty

by

Parker L. Francis

In Partial Fulfillment
of the Requirements for the Degree
Master of Science in
Aerospace Engineering

School of Aerospace Engineering
Georgia Institute of Technology
August 2016

DEVELOPMENT OF THE EVOLVED COMMON HARDWARE BUS (TECHBUS)

Approved by:

Professor E. Glenn Lightsey, Advisor
School of Aerospace Engineering
Georgia Institute of Technology

Professor Brian Gunter
School of Aerospace Engineering
Georgia Institute of Technology

Professor Marcus Holzinger
School of Aerospace Engineering
Georgia Institute of Technology

Date Approved: July 20, 2016

Per Aspera, Ad Astra.

Through hardship, to the stars.

To my family, who has stood by my side these long years in both heart and mind.

ACKNOWLEDGEMENTS

I would like to begin by acknowledging the many people who made this effort possible. It has been a long, arduous journey, but the end is here. I step into my career with a great many experiences behind me. The late nights building spacecraft, the many years learning to be an outgoing professional in all I do, and the adventures that built lifelong friendships have shaped me into who I am today. They will remain the foundation of the person I will become throughout my life and career.

First, my thanks goes to Glenn Lightsey. You have been an excellent advisor, mentor, and enabler of great things over these past years. Your leadership and ambitious endeavours have allowed me to meet many people, work on a number of fantastic projects, and learn a multitude of lessons. I look forward to a long career of partnership with you.

To Andrew and Terry: your antics, groan worthy humor, and simply bad puns made for an excellent lab environment that never left me wanting. One could never call our surroundings dull. On a serious note, you have both made graduate school a great time of learning for me. I could always count on your advice or insight to the numerous challenges I have tackled. We are all three vastly different people in behavior, belief, and skill set, and I believe therein lay our strength.

A special thanks go to Katharine Gamble and Henri Kjellberg for their outstanding leadership and mentorship during our time together in the Texas Spacecraft Lab. You both pushed me to my intellectual limits. You both believed in me, and gave me a frightening amount of authority and responsibility as an undergraduate researcher. I thank you for that opportunity to enrich myself and grow as a leader.

To the many members of the Texas Spacecraft Lab: Juan Ruiz, Alexandra Long, Travis Imken, Shaina Johl, Christopher McBryde, Gokul Anandayuvaraj, Margaret Tam, Jen King, Sean Horton, Karl McDonald, Cody Colley, Macon Vining, Kevin Scholtes, Jesus Charles, Shivani Patel, Ashleigh Caison, David Kessler, and so many more. Thank you all for your

hard work, companionship, and passion for spaceflight. Together we are the driving force behind our generation's need to explore space.

To the members of the Space Systems Design Lab: My time as a yellow jacket was short lived, but I learned an incredible amount at Georgia Tech. I have been greatly inspired by the wide range and complexity of research undertaken by my peers here. I hope to see many of you again as our careers develop.

For the Lightsey Research Group: thank you all for the fun experiences and knowledge exchange we were able to complete. We all have very different backgrounds which allow for us all to grow in various ways. Thomas Choi, Jason Swenson, Tanish Himani, Jian Li, and Swapnil Pujari: you are all in great hands. The LRG has a great future ahead of it, and I cannot wait to see what research comes out of your hard work.

I would like to extend my thanks to Darryl May of NASA's Johnson Space Center for his patience and mentorship. The LONESTAR mission gave me an opportunity that many engineers wait years to have. You not only expanded my understanding of project management, but you have taught me to push forward through adversity and deliver on my commitments. I do hope to work with you again in the future.

The University Nanosatellite Program office of the Air Force Research Labs is owed thanks for the opportunities they offered myself and a number of my peers. The UNP mission is simple: provide students with the opportunity to place a spacecraft in orbit, and teach them spacecraft design and development from concept to operation. The level of passion shown by the students is matched, if not exceeded, by the desire of UNP's staff to teach.

I thank the CalTech Jet Propulsion Lab engineers who brought the RACE spacecraft to life with us at the Texas Spacecraft Lab: Alex Kadesch, Shannon Statham, Jessica Clark, Kenny Donahue, Max Bryk, and Joel Steinkraus. My experience with you (the jepplers) was unique among the other missions we developed at the TSL. Many long nights were spent, and many memories were made. I will always refer to the "packed bacon" in communication system conversations. While our work did not make orbit, I believe we all agree that lessons were learned, and we are all better engineers for it.

Finally, my greatest thanks is owed to my family. They have supported my endeavors throughout life, and made everything I have accomplished possible. To my father Jim, through your example I learned to work hard and believe there is a way to accomplish my goals no matter the obstacles. To my mother Kim, your passion for your career and the love for your family have pushed me to have that same passion for spaceflight while posturing myself to support a family of my own. My many siblings have encouraged me to chase my dreams throughout life, and they have supported me in more ways than they know, even with me living so far away for school.

TABLE OF CONTENTS

LIST OF TABLES

LIST OF FIGURES

SUMMARY

This thesis presents the design and analysis of a small spacecraft bus for use by the Georgia Tech Space Systems Design Lab. It is designed with research projects in mind, and levies the previous design work of The University of Texas at Austin's Texas Spacecraft Lab. The bus offers capabilities that are competitive to currently available commercial small spacecraft busses. The system has been designed with a variety of missions in mind, and is shown to be capable of completing several past missions that each had a customized spacecraft bus. Additional effort was placed into improving the bus' robustness and reliability to a level that has yet to be realized on CubeSats. Redundant components and software algorithms are utilized to ensure system functionality in the event of a component failure. The spacecraft bus has also been developed with the university engineering and research environment in mind. The student-built system's reliability and integrity is developed over the course of many tests, rigorous quality assurance processes, and through the use of heritage flight components. The redundancy and system integration architecture offers an unmatched 98% reliability value for one year missions; this is a 22% increase over typical single-string architectures. Each payload accommodated and each mission flown will add to the bus' heritage as approximately 95% of the spacecraft bus hardware is common between missions. For these reasons, the TECHBus is a novel system that is unique in the current CubeSat bus market, and will provide a powerful platform for space systems research and education at Georgia Tech's Space Systems Design Lab.

DEVELOPMENT OF THE EVOLVED COMMON HARDWARE BUS (TECHBUS)

PART I

Introduction

by

Parker L. Francis

Chapter 1

INTRODUCTION

Over the past decade, the number of university research labs involved in the design, production, and operation of small spacecraft has risen greatly. Access to space for small satellites is at an all time high. In concert with these increases, the missions planned for these platforms have significantly increased in complexity. While university labs are credited with the realization of nanosatellites as a viable science platform, commercial companies have emerged eager to serve the larger scientific and defense research community. In fact, commercial, amateur, and defense satellites accounted for over half of all deployed CubeSat missions since 2013 [1]. Though defense researchers account for the smallest fraction of launches, they have become more interested in small satellite testbeds in recent years.

In the next decade, small spacecraft may take on missions previously intended for larger satellites. Companies like PlanetLabs and Terra Bella are already working toward global imagery updated daily with fleets of CubeSats or nanosatellites [2]. Planetary Resources and a number of other small startups are looking to use small spacecraft beyond Earth orbit for asteroid prospecting. Global web and telecommunications coverage via nanosatellites is a rich business market being pursued by larger companies such as SpaceX. On-demand remote sensing is an emerging commercial market spearheaded by Spire that may be filled by fleets of satellites tasked by the customer [3]. These companies and many more make up the New Space market that is currently redefining the space industry.

As missions are increasing in complexity, payload developers are looking for more robust, dependable spacecraft busses to conduct their flights. Defense researchers are looking toward geostationary orbits to test warfighter technologies, but are hindered by small satellite robustness in the high radiation environment. University researchers at Georgia Tech's SSDL are also looking to fly various payloads of scientific interest without the burden of reengineering the spacecraft bus for each flight.

If university groups intend to participate as hardware providers for these exciting future missions, they will have to continue to innovate to provide rapid development cycles while providing at least commercial industry level small satellite bus performance. The intent of this Master's research is to develop a viable alternative to purchasing commercial small spacecraft busses for the Georgia Tech Space Systems Design Lab. Building upon lessons learned at Dr. Glenn Lightsey's Texas Spacecraft Lab (TSL) at The University of Texas at Austin, a bus design has been developed that addresses a variety of unique challenges that arise in the university setting. The bus offers industry level capabilities in terms of attitude control, payload volume, and science data throughput, but offers system reliability unmatched by commercial alternatives. Because this new bus is developed from the experiences of previous university bus designs, it will be referred to as The Evolved Common Hardware Bus (TECHBus).

The TECHBus offers an in-house solution to the university's need for a platform on which students can be taught the spacecraft systems design process, and new space system research can be investigated. COTS bus solutions, while great for simply executing a mission, can constrain possible avenues for research, and provide no educational advantage beyond teaching integration techniques. The TECHBus is a flexible platform that levies COTS components in order to remove the lower level component design details, while still allowing system level research and payload opportunities that are of more interest to university researchers.

1.1 Contributions

The research in this thesis is intended to create a Preliminary Design Review (PDR) level spacecraft bus design that meets a wide variety of CubeSat research mission requirements. A number of reference missions are utilized as a comparison to benchmark the bus' capabilities. Specific contributions are explained in the following sections. Note that the contributions are tightly coupled and serve to complement one another. In addition to these contributions, the TECHBus design is aimed at providing improvements relative to some commercially available busses in terms of payload volume and mission versatility.

1.1.1 A More Versatile, Reusable Spacecraft Bus

The TECHBus provides a single point design in terms of the core bus required to accomplish a common set of CubeSat research and technology demonstration requirements. Reusability provides cost reduction through the elimination of non-recurring engineering. This contribution continues the work of Gamble and Imken during their time at the Texas Spacecraft Lab [4, 5]. As will be discussed in Chapter 2, the TECHBus is the evolution of the earlier TSL spacecraft bus' component-wise reusable design into a single and completely reusable bus, individual mission payload interfaces aside. This contribution will be quantified via a reusability analysis explained in Section 9.1 and presented in Section 9.2.

1.1.2 Improved Nanosatellite Reliability/Robustness

A number of reliability improvements are implemented by analyzing mission critical functions such as telecommand capability, data downlink, attitude control, etc. Redundancy is incorporated into these critical functions. Components are selected based on reliability metrics or are configured in such a way to improve overall satellite reliability. Furthermore, specific processes and design choices are selected to improve system integrity during the integration, testing, and operations phases. This contribution is tied to the bus' reusability since system testing and heritage for one mission will directly flow down and apply to other missions utilizing the bus. A reliability analysis is performed per MIL-STD-756B, and is presented in Section 10.3.

1.1.3 University Tailored Integration Plan

The TECHBus is intended to be a university platform for space research. It is specifically designed to fit into the educational engineering model of university research labs, though capable of use for the greater aerospace industry. A number of specific university challenges are addressed in Section 2.5. This contribution is broad in the sense that the TECHBus in and of itself helps to mitigate the turnover and loss of knowledge seen at university spacecraft labs. Additionally, specific integration techniques are investigated due to the increased risk posed by university student technicians, thus increasing system reliability. The effect of

integration processes and techniques are difficult to track and quantify. However, those that are specific to hardware design choices are captured in the reliability analysis (e.g. reducing the total number of wire connections). Understanding how to quantify quality assurance processes is an ongoing area of research throughout the industries that involve manufacturing and production [6].

1.2 Thesis Organization

This thesis comprises 3 parts and 12 chapters. Part 1 introduces the research and provides a history of the Lightsey Research Group. Part 2 contains the design chapters of the TECH-Bus, and Part 3 compares the TECHBus against commercially available busses. Chapter 2 provides an overview of the CubeSat Standard, and the Lightsey Research Group's previous work as it relates to this thesis. Chapter 3 presents an overview of the TECHBus architecture. The bus' various subsystems are presented in detail with a narration of the design reasoning for each decision in Chapters 4 through 7. Chapter 8 contains a description of the TECHBus' system design with respect to how each subsytem is integrated together into a cohesive spacecraft. An in-depth comparison of the TECHBus against the TSL heritage CubeSat bus and other commercial busses is presented in Chapters 9-11. The comparison examines reusability between missions, spacecraft reliability, and payload capabilities. Chapter 12 summarizes the research presented, and provides suggestions for future work in this area.

Chapter 2

BACKGROUND

The following chapter will review a variety of topics that lay the background for the TECH-Bus' motivation and design choices.

2.1 The CubeSat Standard

The CubeSat is a standardized small satellite form factor originally created by California Polytechnic State University (CalPoly) and Stanford University in 1999 [7]. Along with defining the standard itself, CalPoly developed the Poly Picosat Orbital Deployer (P-POD) as a container for attaching CubeSats to launch vehicles as secondary payloads. This containerized launch configuration has led to the growth in launch opportunities for CubeSats due to the reduced risk posed to the primary payload. The CubeSat Standard calls for spacecraft designed on a unit (U) scale where 1U is equivalent to a 100.0 x 100.0 x 113.5 millimeter volume with a maximum mass of 1.333 kilograms [7]. Since its inception, the standard has been adapted to allow for various sizes such as 1.5U, 2U, 3U, and most recently, 6U and 12U spacecraft.

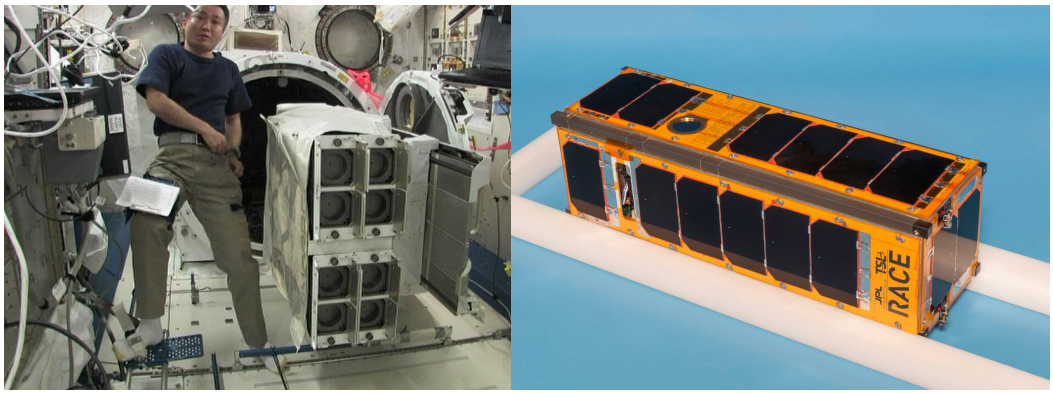

Figure 1: NanoRacks 48U deployment system (left), RACE 3U CubeSat (right).

At the time of writing this thesis, the CalPoly P-POD has yet to be adapted to sizes other than 1U and 3U CubeSats. However, a number of companies have emerged in the

deployer market with their own variations on the standard. Innovative Solutions in Space (ISIS), NanoRacks, and Planetary Systems Corporation (PSC) are companies of note in the launch adapter domain. NanoRacks has successfully established an International Space Station (ISS) partnership with their deployer seen in Figure 1 that has arguably made the most impact in CubeSat access to space. With every NanoRacks populated ISS resupply mission, the company can place up to 48U worth of CubeSats in orbit. PSC's launch vehicle history reaches back to 2001 with the Lightband separation system utilized by both primary and secondary payloads [8]. In 2012, PSC developed their Canisterized Satellite Dispenser (CSD) which is currently the only 6U satellite deployer currently commercially available [9]. ISIS has developed the ISIPod which is the leading CubeSat deployer for non-US launch vehicles, and comes in 1U, 2U, and 3U sizes. Because of the recent growth in CubeSat launch access, and the outlook for even greater access, the TECHBus has been developed to be consistent with the CubeSat Standard [10]. This includes both 3U and 6U form factors with the option to scale to larger form factors in the future. The design tries to best meet the standards developed by all four commercial deployer providers: CalPoly, PSC, NanoRacks, and ISIS to provide a wide range of options for obtaining access to space.

2.2 Lightsey Research Group

The Lightsey Research Group (LRG) is composed of university students under the instruction of Dr. E. Glenn Lightsey now at the Georgia Institute of Technology (Georgia Tech). The research conducted by the LRG focuses primarily on spacecraft technology, including spacecraft design, development, and operation. This includes related topics such as: guidance, navigation, and control algorithms; formation flying and satellite swarms; proximity operations and autonomous rendezvous; space based Global Positioning System receivers; visual navigation; 3D printed propulsion; and space systems engineering. The LRG emphasizes flight projects as a motivation for conducting new research and as a means to demonstrate new capabilities. The LRG participates in the entire flight project life cycle, including proposal, mission design, hardware and software design, assembly, integration, test, launch, in-flight operations and post mission analytics.

2.2.1 The Texas Spacecraft Lab CubeSat Bus

Prior to moving to Georgia Tech in 2015, the Texas Spacecraft Lab (TSL) was initially established in 2003 as a part of the LRG at The University of Texas at Austin (UT-Austin). The TSL designed, developed, and operated a number of small spacecraft. At the time of this thesis, the TSL has launched and operated four university designed and built small spacecraft in Low Earth Orbit (LEO): FASTRAC-1, FASTRAC-2, Bevo-1, and Bevo-2. Another TSL spacecraft known as RACE was completed and delivered to the California Institute of Technology, but was destroyed in the Orbital Resupply Mission 3 (Orb-3) launch vehicle failure in 2014. The final TSL mission, ARMADILLO, is currently on schedule for a late 2016 delivery and 2017 launch aboard the US Department of Defense's Space Test Mission 2 (STP-2). In addition to these six spacecraft, the TSL has developed a number of other system designs for proposals, and delivered a number of separate subsystems for other commercial and scientific small satellites.

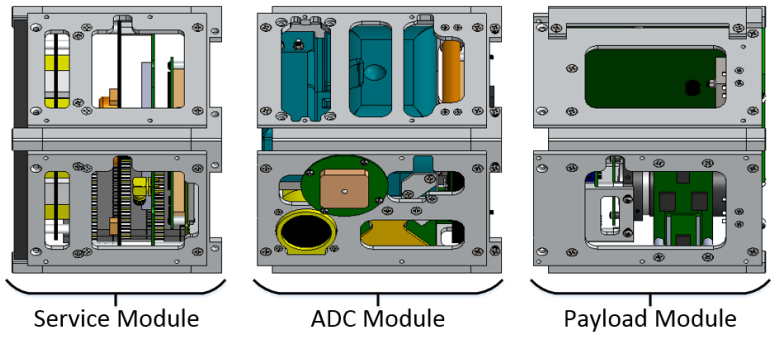

Figure 2: TSL CubeSat modular design.

After the delivery of the Bevo-1 spacecraft, the TSL sought to develop a CubeSat bus that would leverage common components across mission designs to reduce Non-Recurring Engineering (NRE) cost. The efforts of Gamble and Imken led to the creation of the TSL 3U CubeSat Bus, which was implemented on the Bevo-2, RACE, and ARMADILLO CubeSats [4, 5]. The design consisted of a modular structure that simplified the integration and testing process. The Service Module existed at one end of the spacecraft with the Payload Module at the other. Between the Service and Payload Module was the Attitude Determination and Control (ADC) Module. The module organization is depicted in Figure 2. The

segmentation of the spacecraft into functional modules allowed for a simpler hardware integration process than before, and added an intermediate point for hardware testing. Each module could be independently tested as a standalone unit prior to integration with the others, which simplified spacecraft assembly and testing. Each module included a section connector and/or endcap that mated to the adjacent module's shell. The shell became the primary structure for the modules by creating a housing for the components, a mounting point for external sensors, and a face to affix the solar panels. Examples of these two components are given in Figure 3.

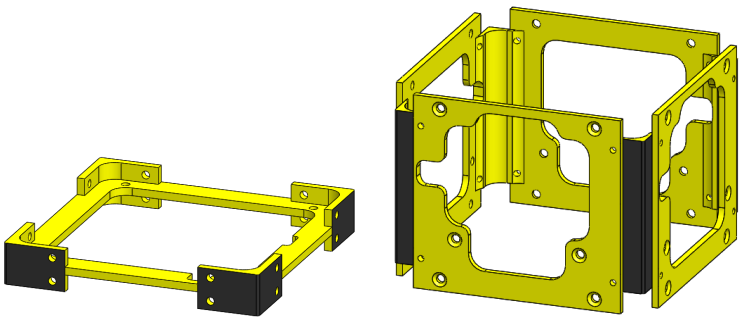

Figure 3: TSL CubeSat Bus section connector (left), and shell (right).

The Service Module contained the satellite's primary systems such as the Command and Data Handling System (CDH), a UHF/VHF full duplex radio and deployable antenna, and the Electrical Power System (EPS). The ADC Module contained the sensors and actuators required for 3-axis control of the spacecraft, though RACE was a spin-stabilized spacecraft with only magnetorquers and a single reaction wheel. Sun sensors, MEMS gyroscopes, and a magnetometer made up the sensor suite utilized on the TSL bus. Actuators consisted of a triad of magnetorquer rods and reaction wheels. An in-house developed cold gas thruster was also included for the Bevo-2 mission. The Payload Module was reserved for each mission's unique payload instrument and a GPS receiver if required.

2.2.2 Previous Missions

Three missions designed by the LRG at UT-Austin used the TSL CubeSat Bus. Since the TECHBus design builds upon lessons learned from the TSL Bus implementation on these

missions, a brief description of each mission is presented.

2.2.2.1 Bevo-2

The Bevo-2 mission, launched in February 2016, is the follow-on to the Bevo-1 spacecraft which was launched in 2009. Both of these missions are part of the Low-Earth Navigation Experiment for Spacecraft Testing Autonomous Rendezvous and Docking (LONESTAR) program; a partnership between UT-Austin, Texas A&M University, and NASA Johnson Space Center. The partnership was established to explore and develop new Autonomous Rendezvous and Docking (AR&D) systems for use on low power microsatellite infrastructures [11]. Under the original concept, the two universities were to develop four pairs of cooperative spacecraft over four missions to implement and demonstrate these AR&D technologies. To date, two of these missions have been completed.

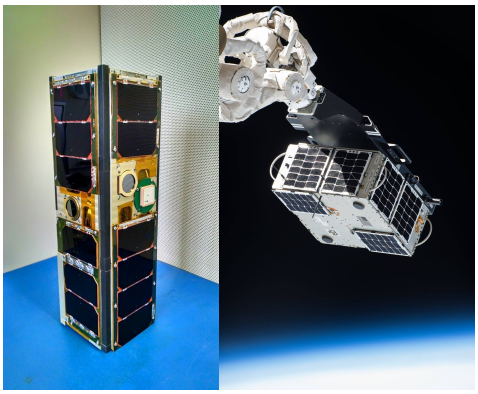

Figure 4: Bevo-2 spacecraft (left), AggieSat-4 spacecraft (right).

Bevo-2 is a 3U CubeSat with 3-axis attitude control additionally equipped with a single-axis cold gas propulsion system for limited proximity maneuvers. AggieSat-4 (AGS-4) is a 50 kilogram nanosatellite equipped with 3-axis attitude control and a custom ISIPod in which Bevo-2 is stowed. Both spacecraft are equipped with crosslink radios to demonstrate cooperative relative navigation technologies. Bevo-2 and AGS-4 were launched to the ISS aboard the Orbital Resupply Mission 4 (Orb-4 or OA-4) launch vehicle on December 6, 2015. The pair of spacecraft were deployed on January 29, 2016 from the ISS via the Cyclops nanosatellite deployer. Following a 31 day safety period, Bevo-2 was to be deployed from AGS-4 to begin the relative navigation portion of the mission.

Due to schedule, programmatic, and hardware problems, the Bevo-2 CDH software lacked a functional radio beacon. This made tracking the spacecraft difficult after its deployment because the spacecraft will only respond upon the receipt of a valid ground command. At the time of publishing this thesis, only limited contact with the satellite has been made. FlatSat testing and ground-based troubleshooting points to a flight radio hardware problem as the most likely cause for the lack of communications.

2.2.2.2 ARMADILLO

The Atmospheric Related Measurements and Detection of Submillimeter Objects (ARMADILLO) mission is a part of the University Nanosatellite Program's (UNP's) 7th competition cycle that started in 2011. It was selected as the CubeSat class winner at the Flight Competition Review in January 2013. ARMADILLO's primary scientific objective is to characterize the submillimeter dust debris environment in orbit with an in-situ detector developed by Baylor University. The spacecraft is also equipped with a dual-frequency GPS receiver intended for measuring ionospheric total electron content using the spaceborne GPS radio occultation technique. A retroreflector payload was added to the mission in 2014 for ground based laser ranging. The ARMADILLO bus is identical in capabilities to Bevo-2 with the exception of not containing the cold gas propulsion unit.

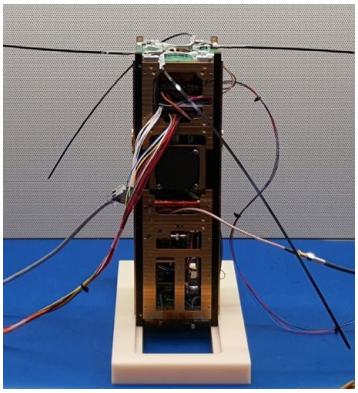

Figure 5: ARMADILLO spacecraft during day-in-the-life testing.

ARMADILLO is scheduled for delivery to the Air Force Research Labs in Summer 2016 for environmental testing. It is manifested for launch aboard the Space Test Program 2 (STP-2) flight which is currently scheduled to occur in early 2017. Since UT-Austin is not

supporting the mission past vehicle delivery, ground operations for ARMADILLO will be conducted by Georgia Tech using their own satellite ground station.

2.2.2.3 RACE

The Radiometer Atmospheric CubeSat Experiment (RACE) mission was a partnership between the TSL and the California Institute of Technology (CalTech) Jet Propulsion Lab (JPL). The payload was a 183 GHz radiometer engineered by JPL to demonstrate a newly developed miniaturized instrument. The RACE bus was configured with a simplified ADC Module for a spin stabilized operating attitude. The activity was initiated in April 2013, and the flight spacecraft was delivered to JPL for environmental testing in February 2014 resulting in an 11 month turnaround time from mission start to flight unit delivery.

The RACE spacecraft was delivered to NanoRacks for an ISS deployment and intended launch aboard the Orbital Resupply Mission 3 (Orb-3 or OA-3) on October 28, 2014. However, due to a catastrophic launch vehicle anomaly and failure, the CubeSat never reached orbit.

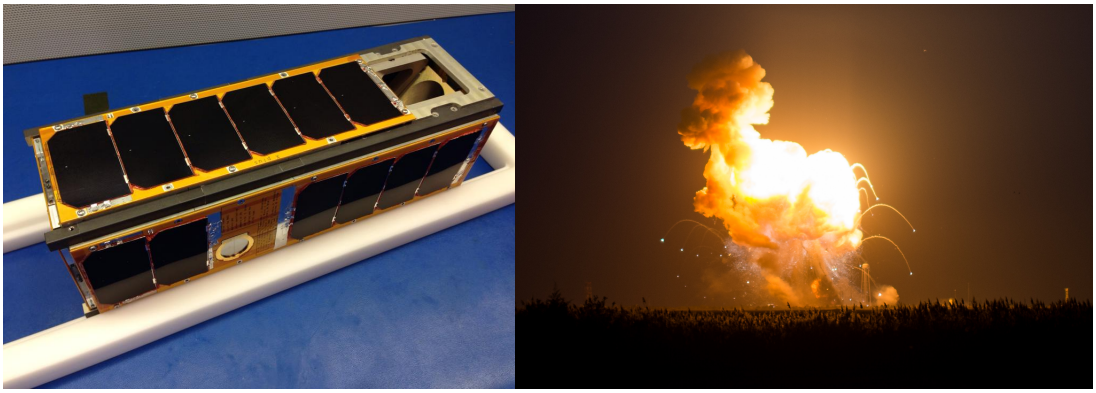

Figure 6: RACE spacecraft (left), Orb-3 launch failure (right).

2.2.3 Future Missions

In addition to the historical missions discussed in the previous section, a number of new missions are currently being planned by the LRG at Georgia Tech. MicroNimbus is a future CubeSat mission with a payload developed by the Georgia Tech Research Institute (GTRI). The GTRI partnership with the LRG will form the basis for a 3U CubeSat using

the TECHBus design to achieve sub-degree pointing accuracy. The payload is a 60 GHz radiometer roughly 1U in size that will profile the Earth's atmospheric temperature. The mission is a technological successor to the Nimbus series of US meteorological research spacecraft. Much of the work presented in this thesis directly applies to the design, systems engineering, and operation of the MicroNimbus spacecraft.

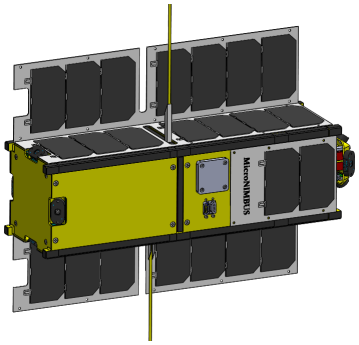

Figure 7: MicroNimbus spacecraft preliminary design.

2.3 The Spacecraft Life Cycle

Spacecraft missions are managed in a number of ways across the aerospace industry. The LRG typically works with the NASA Life Cycle Phases scheme which is described in this section. The definition and guidelines for this life cycle are given in NASA Procedural Requirements document NPR 7120.5D [12]. Figure 8 presents the NASA Life Cycle Phases in a timeline format.

At the most abstract level, a space mission is split into *formulation* and *implementation* parts. The formulation phases determine mission feasibility, define the project goals, dictate system requirements, and plan out acquisition strategies. The implementation half takes these inputs and produces a design, manufactures, integrates, tests the space vehicle(s), and then launches and operates the mission.

In further detail, the project formulation consists of two distinct phases referred to as Phase A and Phase B. Phase A consists of evaluating mission concepts, and developing the technologies required to complete the mission. Some institutions conduct Pre-Phase A operations through concept studies to explore whether or not various mission concepts

are even feasible. Phase B is where concepts are transformed into preliminary vehicle designs, and required technologies are demonstrated as ready for implementation. Component acquisition strategies are assembled, and the project sees its first major review: the Preliminary Design Review (PDR). PDR is typically a key decision point where stakeholders and sponsors come together and either approve or decommission a project.

The first phase of implementation begins after project approval, and is referred to as Phase C. Phase C is composed of final design and the Critical Design Review (CDR). Success at CDR usually results in moving to manufacturing and procurement of vehicle components. Some limited procurement may occur before CDR for long-lead items if the institution has confidence the project will be approved for implementation. The next phase, Phase D, consists of system integration, testing, operations planning, and launch.

Phase D may very well be the most crucial point in any spacecraft mission. Appropriate quality assurance processes are required to ensure integration goes as planned, and sufficient testing is completed to guarantee mission success. A mishap during Phase D may very well kill a mature program with millions of dollars invested in it.

Two important reviews generally occur during Phase D: the Operational Readiness Review (ORR), and Flight Readiness Review (FRR). The ORR examines the operations team's readiness for vehicle checkout and nominal operations on orbit. This involves nominal procedures as well as fault or anomalous behavior plans. After a successful ORR, FRR is completed to review the vehicle's readiness for flight. FRR is the last key decision point before the spacecraft is integrated with its launch vehicle and placed in orbit.

Phases E and F follow the launch. Phase E is the operations phase, and consists of executing the entirety of the mission planned in Phase A. Various reviews may arise for critical points in the operational schedule such as aperture deployments, instrument calibrations, and the initiation of nominal operations. After the operations phase has concluded, Phase F begins with the end-of-life process for the space vehicle (safe parking orbits, forced deorbit, failed launch, etc.), and continues with documentation of various project processes, results, and operational data. A decommissioning review is typically conducted prior to the final archival of data.

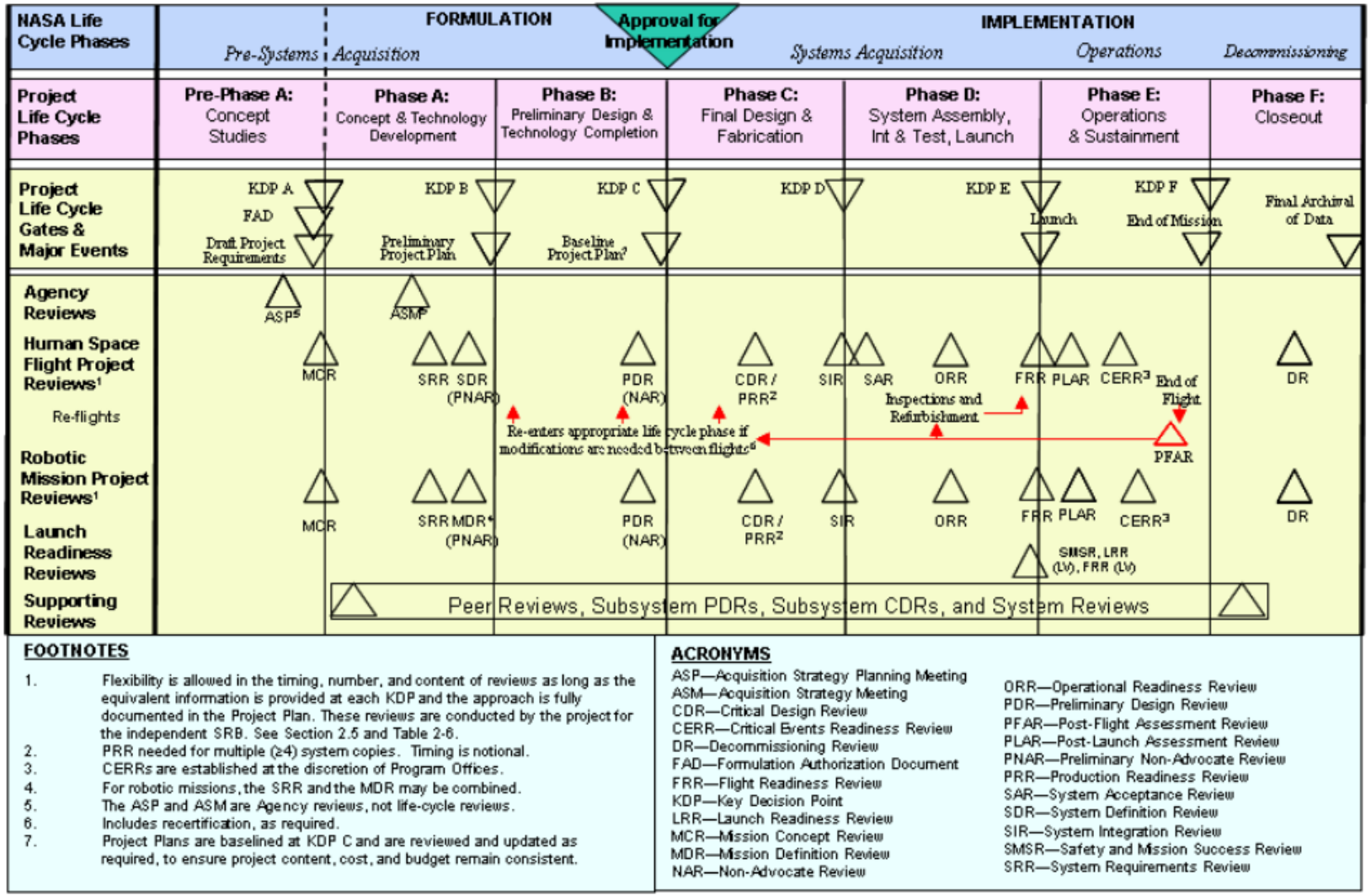

Figure 8: NASA Life Cycle Phases.

With the project life cycle explained, it is important to indicate that the TECHBus is notionally a Phase B design. While it truly straddles the border between Phases B and C, no fabrication has been completed to date. Components and providers have been selected, and are described in the following chapter. However, a suitable payload design and complete mission plan would be required to justify Phase C placement. The MicroNimbus mission previously mentioned is intended to serve as a Phase C example of the TECHBus' implementation.

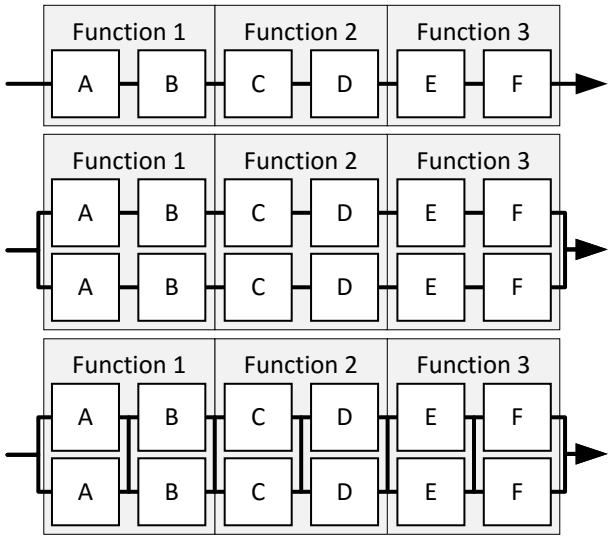

Figure 9: Redundancy architectures: single string (top), dual string (middle), and cross-strapped (bottom).

2.4 Spacecraft Reliability

Reliability can be greatly increased by designing redundancy into systems through the use of backup components. A system without redundancy is referred to as *single string,* and is the case for most small spacecraft designs. A system with a completely redundant string in parallel to the primary is referred to as *dual string* or *large scope redundant.* Finally, a system in which all components are in parallel to their backup counterpart is referred to as *cross-strapped* or *small scope redundant.* Figure 9 shows an illustration of each system design. Each architecture has advantages and disadvantages when viewed from a programmatic

standpoint. Cross-strapped systems offer the most operational flexibility, but induce more engineering cost than a dual string design. Additionally, adding redundancy to any system increases budget and volume costs. For this reason, most low budget and volume constrained small spacecraft missions forego any redundancy. It should be noted that programs may combine various architectures across the system in order to best serve their mission and program profile. An extensive discussion of calculating reliability metrics for components and systems is presented in Sections 10.1 and 10.2.

2.5 The University Spacecraft Engineering Environment

Various challenges arise in university spacecraft labs that may not generally exist in industry. First and foremost, university labs must combat knowledge loss and turnover. Students graduate each year, and take with them the experience they gained. However, it can be difficult to make sure that experience is passed along to younger students. Attempts have been made to create training sessions, to document lessons learned, etc. Unfortunately, university students are often short on time, and cannot be expected to complete these efforts in an adequate manner. In an ideal world these solutions are obvious and simple to execute, but the university setting is not ideal and experience from the Texas Spacecraft Lab has shown they are not sufficient.

Beyond knowledge loss, simple inexperience of student technicians can bring about a risk to the mission they are working on. Training and mentorship by veteran students is often required before flight components can be worked with, but even experienced students make mistakes. They cannot be expected to perform at the level of industry technicians who have 20 years of experience at their trade.

To mitigate these two risks, the TECHBus design incorporates modifications intended to reduce technician risk, which are combined with recommendations for managing a university lab. The bus design architecture of the TSL bus is evolved to allow simpler de-integration of the spacecraft through a half-shell structure. This simple modification, in addition to reducing cost, enables access for students to repair mistakes or re-route electrical harnesses, for example, without complete disassembly of a spacecraft module. Effort was also placed

into reducing the overall number of electrical harnesses required. Each crimp is a failure point that is easy to incorrectly install. Additionally, the redundancy of the bus, while generally intended to improve small spacecraft reliability, also serves to mitigate the risk imposed by student technicians. The failure of a single component is no longer catastrophic to the mission's success. As a more general mitigation technique, the TECHBus in and of itself serves to maintain knowledge over a number of years and reduce the amount of non-recurring engineering completed in a university lab. For every mission the system is built for, a more thorough understanding of the system is gained, and processes can be iterated and improved upon. The uncertainty of a completely new integrated system for each mission is removed from the development process.

Managing a university lab is a significant undertaking, and requires a lot from the graduate or undergraduate student(s) charged with doing so. From direct experience, the amount of work completed and the quality at which it is completed stems directly from the student manager's effectiveness at holding other students accountable, and encouraging them to do everything to their utmost ability. Some students are natural leaders. They can be capable of taking a university spacecraft lab from a concept to a renowned source of spacecraft busses throughout the industry. That said, they are still students and must split their attention in order to continue their own educational career. Furthermore, it is common for student managers to become frustrated as they carry all of a mission's responsibility, but with little to no authority. With the experiences of the Texas Spacecraft Lab and Space Systems Design Lab taken into account, the most effective way to run a university lab with the utmost confidence in the quality of work performed, and the confidence to meet commitments, is to hire a full time employee to manage day-to-day activities.

A full time Lab Manager, be it an engineer or post-doctorate, can focus 100% on the tasks at hand. This creates a single point of management for the lab, and allows for a more organized execution of the spacecraft development process. The Lab Manager can be the knowledge retention for a lab who loses students each year. Training sessions become less work to the veteran students, quality assurance processes can be organized and streamlined, and both responsibility and authority can be charged to the Lab Manager.

It is recognized that many university labs will not have the resources necessary to hire a full or even part-time Lab Manager in their early years. In this case, the lab must have strong involvement from its Principal Investigator with a small group of highly motivated student leaders. This management team must be effective at delegating the necessary tasks among one another, and to the students working at the subsystem level. The design of a spacecraft is a complex project management challenge as much as it is a technical one. Most engineering schools now offer engineering management plans. Diversifying the student workforce in a university spacecraft lab is important, and these programs offer an excellent resource in terms of lab management. The same concept applies to recruiting students from a wide range of engineering programs in order to effectively solve the problems presented by the multidisciplinary task of spacecraft design.

DEVELOPMENT OF THE EVOLVED COMMON HARDWARE BUS (TECHBUS)

PART II

The Evolved Common Hardware Bus (TECHBus)

by

Parker L. Francis

Chapter 3

ARCHITECTURE OVERVIEW

At the most general level, the TECHBus architecture can be described as a common hardware bus that requires limited mission customization (i.e. payload mechanical and electrical interfaces). It is important to be clear that the TECHBus will not satisfy every mission. There will always be payloads that require a truly custom spacecraft bus or go beyond the capabilities of the TECHBus, but this architecture is intended to accommodate a wide range of CubeSat mission profiles.

The TECHBus architecture builds upon that of the TSL CubeSat bus. The Service, ADC, and Payload module architectures will remain, though the ADC module will move to the top of the 3U structure. This allows for simpler payload interfacing to the CDH flight computer, and removes the need for payload data/power lines to pass through the ADC module where electromagnetic interference could complicate transmission. The TECHBus ADC also employs the "tuna can" or "3U+" volume allocated at the top of the 3U structure by the CalPoly CubeSat Standard Revision 12 [13]. The Service module occupies the center of satellite such that interfaces to both the ADC and Payload are concise and simple. The Payload module remains at the end of the bus. This configuration allows for more options with respect to payload apertures.

The 6U TECHBus is designed to retain the modular form factor although the structural design prevents the same 3U implementation. Instead, components are integrated to secondary structure where module based testing can still be completed. After this testing phase, the subassemblies are integrated into the primary structure. The Service stack components occupy a corner of the 6U volume with the ADC components installed next to them. The Payload volume is separated by a structural bulkhead, and occupies the remaining 4U space. Illustrations of both the 3U and 6U TECHBus' are given in Figure 10.

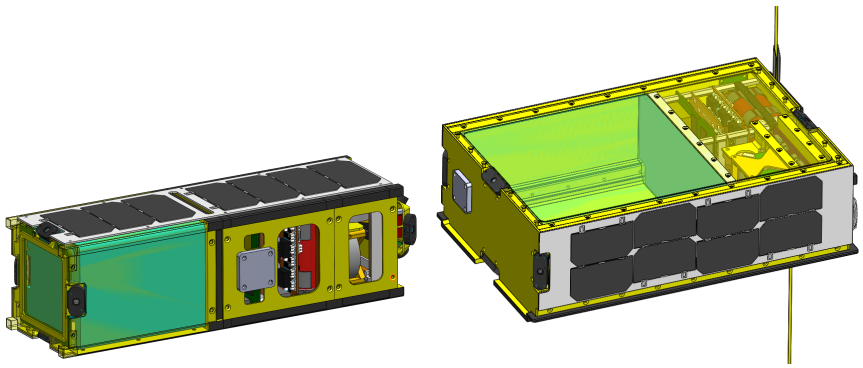

Figure 10: 3U TECHBus (left), and 6U TECHBus (right) with payload volumes highlighted in green.

Increasing the survivability and reliability of the TSL bus is a key design goal for the TECHBus. This is achieved through selective redundancy, the use of known reliable hardware components and providers, and a radiation tolerant flight computer. The discussion of redundancy is unique to each component on the bus based on its failure likelihood and the difficulty of implementing a redundancy plan. Each subsystem's unique redundancy architecture is addressed in its following section.

As a general overview, the 3U and 6U TECHBus both implement a 3-axis ADC module that utilizes sun sensors, magnetometers, and body rate gyroscopes for attitude determination (with a star tracker option), and magnetorquers and reaction wheels for control. The spacecraft bus' service module houses a lithium ion battery pack and power distribution system, both low and high data rate radios, a multi-constellation capable Global Navigation System Satellite (GNSS) receiver, and a single flight computer for both CDH and ADC processes. The payload interface is customized and implemented via a single PCB at the junction of the Service and Payload modules.

Chapter 4

COMMAND AND DATA HANDLING DESIGN

The Command and Data Handling (CDH) system is one of the most important subsystems on any spacecraft. It is charged with taking instructions from ground operators and turning them into actions performed by the various subsystems, and managing the vehicle's status telemetry and payload data for downlink. A CDH failure usually means the end of the mission. Because of this, the CDH selection for TECHBus is of utmost importance. Radiation tolerance is particularly important as the number of high altitude, interplanetary, and long duration CubeSat missions is expected to increase.

CDH architectures generally fall into three categories: *centralized, distributed,* and *federated*. A centralized CDH is described by a single flight processor connected directly to each other spacecraft device. A distributed CDH has a single processor connected to a unified communications protocol bus (e.g. MIL-STD-1553 bus). Each other spacecraft component is also connected to the same bus, thus allowing for inter-component communication without the need for flight computer interaction. Finally, a federated CDH architecture is related to the distributed CDH, but with multiple flight processors. This allows for distribution of the CDH workload across multiple computers and improved system reliability if implemented with fault tolerant software design [14]. Figure 11 illustrates the centralized and distributed architectures.

COTS systems-on-a-module (SOM) are often designed to be compatible with a wide range of communication protocols and busses. This allows for simple interfacing with a number of devices that likely have differing communication schemes. The TECHBus will leverage this capability with a COTS SOM, and implement a centralized CDH architecture. While a federated redundant CDH would prove more reliable, the use of multiple CDH processors levies too much cost in size, weight, and power to justify. Instead, a radiation tolerant processor has been pursued to make up for the potential loss of reliability.

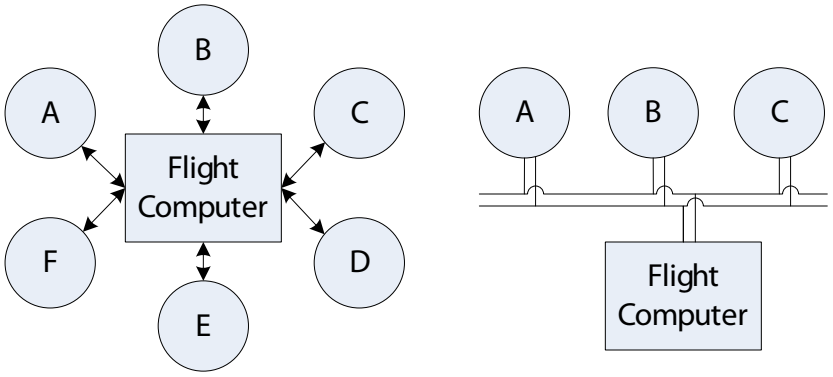

Figure 11: CDH architectures: centralized (left), distributed (right).

4.1 Command and Data Handling Component Trades and Selection

Since 2015, the LRG has been working with the UNIBAP heterogeneous computing unit produced by Bruhnspace Advanced Projects as a candidate for the TECHBus CDH flight computer. This SOM is designed specifically for "safety critical, radiation tolerant" applications by using "optimized heterogeneous parallel algorithms" that utilize both an AMD CPU and an ARM FPGA [15]. The device employs a small form factor with high performance characteristics. The UNIBAP CPU runs at nearly 12 times the speed of the TSL CubeSat Bus' previous CDH processor: the Phytec LPC3250 SOM. Furthermore, it has over 30 times as much RAM on board as the LPC3250 [16]. Drawbacks of the unit include relatively high power draw (roughly five times that of the LPC3250) when both the CPU and FPGA are running. However, the unit still fits within the PC/104 board standard and is therefore a viable CubeSat option. A comparison of the two SOMs is given in Table 1. Based on the performance characteristics of the FPGA, that side of the UNIBAP has been baselined for nominal operations. The AMD will be powered on based on payload processing needs only.

Table 1: Flight computer technical comparison.

CPU	Clock Rate [MHz]	RAM [MB]	NAND [MB]	Power Draw [W]
LPC3250	208	64	64	1
UNIBAP	2,400	2,048	4,096	2

The UNIBAP makes use of novel radiation protection circuitry, making the FPGA operationally impervious to Single Event Latchups (SELs). SELs are radiation events in which transistors that make up chip level components become latched into a shorted state. While the UNIBAP is operationally immune to these events, the physical transistors do in fact latch. A sign of latchup events is increased overall current draw by the device. The UNIBAP's FPGA health monitoring system tracks this metric, and informs the flight software (and/or ground operators) when a reboot is required to clear the errors.

A variety of development advantages come along with the UNIBAP system. The SOM runs an embedded Linux environment (as did the LPC3250). However, the UNIBAP kernel carries onboard compiling capabilities that allow for direct development on the flight computer itself rather than cross compiling software written on a desktop computer. This direct link to the operating system reduces potential cross compiling errors that can reduce software robustness. Software testing on the device is also simplified since there is no requirement for additional testing equipment to access the CDH within the spacecraft (e.g. a host terminal computer). Finally, the UNIBAP's high CPU clock rate allows both the CDH and ADC operations to be co-located on the same flight computer. This removes the need for a second flight computer thus reducing cost, power, and volume needs for the TECHBus while improving reliability.

Radiation tolerant NAND memory has been selected for use with the UNIBAP to guarantee the integrity of the full data handling chain. Standard NAND memory is susceptible to radiation events such as single-event upsets, single-event latchups, and stored memory bit flips. The UNIBAP architecture's advantages would mean little without radiation tolerant data storage in preparation for downlink. The NAND module selected for use on the TECHBus' CDH is rated to 50 kilorads of Total Ionizing Dose (TID) [17], and is depicted in Figure 12. TID measures a component's lifetime resilience to radiation exposure which will decay its performance over time. Standard COTS electronics are often rated to only 5-20 kilorads [18]. While the continued miniaturization of radiation tolerant/hardening is cutting edge, the module selected for use on the TECHBus benefits from over a dozen years of flight heritage without failure [19]. The TECHBus CDH will fly 4 gigabytes of NAND

memory in its standard configuration with the capability to expand as payload needs dictate. Additional memory could be configured onto the Payload Interface Board (described in Section 8.1.3).

Figure 12: Radiation tolerant NAND chip [17].

4.2 CDH System Summary

The TECHBus CDH uses a centralized processor architecture. The flight processor is a radiation tolerant heterogeneous computing unit, and handles processing for both the CDH and ADC software. Flight data will be stored for downlink in radiation tolerant NAND memory that has seen significant use on orbit. The TECHBus CDH design is an improvement over the TSL bus' CDH in a variety of ways, and should prove to be a much more robust and reliable subsystem.

Chapter 5

ATTITUDE DETERMINATION AND CONTROL DESIGN

Attitude determination and control subsystems enable many spacecraft missions that would otherwise be impossible with a passive, tumbling vehicle. Even though some missions could potentially be completed without attitude control, attitude knowledge is almost always necessary to post-process science measurements into meaningful data. The ADC is responsible for resolving the vehicle's inertial orientation, stabilizing the body rates, and often providing active spin or pointing control.

Sensors utilized for attitude determination fall into two categories: internal (or inertial), and external sensors [20]. Internal sensors measure quantities like rotational and linear accelerations with gyroscopes and/or accelerometers, respectively. This direct measurement of the system dynamics is important where analytic dynamic models are complicated, unavailable, or inaccurate. Internal sensors allow for attitude propagation during gaps between external sensor measurements. External sensors provide a reference in the vehicle's inertial frame by which to deduce a single point measurement of the vehicle's attitude. These external references also allow for adjustments in the propagation of the system's dynamics due to inertial sensor drift. Examples of external sensors include star trackers, sun sensors, magnetometers, horizon sensors, etc. In general, spacecraft ADCs are equipped with both internal and external sensors that work together within an optimal state estimator such as a Kalman filter.

An ancillary sensor that does not directly provide attitude information is a GNSS receiver. However, GNSS receivers are critical for a variety of reasons. They provide information to correlate orbital position to science data. Furthermore, they prove an accurate, absolute time reference and enable the use of lookup models for the magnetic field, Sun or Moon ephemerides. Spacecraft without GNSS receivers must resort to the use of uplinked ephemerides to predict its position throughout its orbit, and are susceptible to integration

error based on the update interval, orbital model fidelity, and lack of an accurate time reference.

For active attitude control, ADCs implement a variety of actuators to impart torques on the spacecraft. Much like sensors, actuators fall into internal and external torque groups [20]. Internal actuators (e.g. reaction/momentum wheels, control moment gyroscopes) create torques that change the vehicle's body rates, but do not alter the body's total angular momentum vector. External actuators (e.g. thrusters, magnetic torque rods), however, do alter the vehicle's angular momentum vector, and are often used to desaturate or load internal momentum actuators.

The attitude determination and control system for the TECHBus relies heavily on work previously completed by the TSL at UT-Austin. A completely functional ADC was developed and tested at the TSL, and is being flight demonstrated on the Bevo-2 and ARMADILLO CubeSats. The goals for the TECHBus system iteration are to improve reliability, operational constraints, and performance capabilities.

Reliability improvements for the ADC focuses on high risk items such as the Inertial Measurement Units (IMU) and reaction wheels. In the TSL bus design, failure of either of these components would result in complete loss of spacecraft control. As such, component redundancy has been implemented to ensure at least one fault tolerance to the primary mission objectives.

Redundant IMUs are paired together, while reaction wheel redundancy is implemented via software. It is argued that, for the CubeSat form factor, the power, volume, and cost impact of adding a fourth reaction wheel outweighs the need for hardware redundancy. Instead, unique guidance and control algorithms are implemented to remove the need for additional hardware. A satellite can achieve three axis control with only a pair of reaction wheels (though at some performance cost). The TSL bus included two digital sun sensors. While two sensors achieves redundancy with some additional operational constraints, the TECHBus increases the number of sensors to increase redundancy and remove constraints on nominal operations.

5.1 Attitude Determination Component Trades and Selection

Several sensors are presented below. Each was selected on the basis of enabling attitude determination for complex small spacecraft missions, component reliability, and lessons learned from the TSL CubeSat bus. The TECHBus is equipped with a pair of inertial measurement units that house three-axis gyroscopes and accelerometers, and magnetometer is integrated for measuring the Earth's magnetic field. Sun sensors are utilized as the primary external sensor. An optional star tracker can be included for the most demanding missions.

The VectorNav VN-100 IMU was selected for use on the TECHBus. The unit houses a three-axis gyroscope, accelerometer, and magnetometer within a compact form factor. On the TSL bus, each of these three sensors were independent of one another and resulted in significantly more development cost than a single integrated IMU. The VectorNav's compact size allows for two units to be easily used in a redundant manner without incurring significant volume cost to the bus. In addition to their more efficient use of volume, the VectorNav offers excellent performance in comparison standard MEMS sensors with regard to angular random walk and bias stability. The VN-100 recently flew aboard the AggieSat-4 microsatellite.

Figure 13: VectorNav VN-100 IMU (left) [25], Sensonor STIM300 (right) [27].

In order to provide greater attitude knowledge capabilities on the 6U TECHBus, an IMU was selected with better stability and resolution. The Sensonor STIM300 device was selected for its greater accuracy while still maintaining a form factor small enough for use on

a 6U CubeSat. However, the unit is too large and draws too much power to be considered for use on a 3U bus where redundant sensors are desired. Furthermore, the STIM300 lacks an integrated magnetometer meaning additional volume and power is required to accommodate another sensor. The 6U TECHBus will fly a STIM300 as its primary IMU, with a VectorNav serving as a backup. This configuration maintains the bus' redundancy while providing a more capable ADC for nominal operations.

The Honeywell HMR2300 is used as the primary magnetometer on the 6U TECHBus to maintain redundancy, and offer an improvement in resolution of the VectorNav's magnetometer. This sensor has been flown on each of the TSL CubeSat bus' spacecraft, and provides very accurate measurements of the Earth's magnetic field. Magnetometers prove invaluable for implementing coarse attitude determination, or control when equipped with magnetic torque rod actuators.

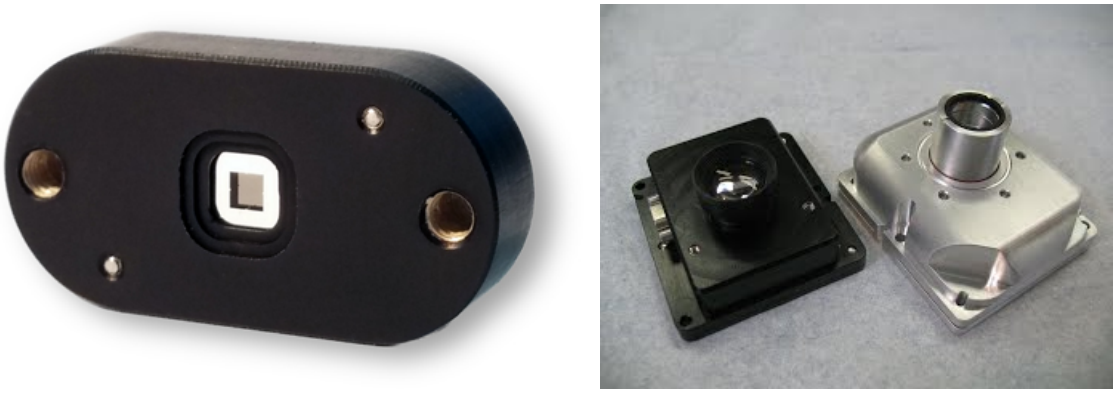

Figure 14: SolarMEMS NanoSSOC sun sensor (left) [24], Sinclair Interplanetary ST-16 (right) [21].

The primary external sensors for both 3U and 6U models of the TECHBus are the SolarMEMS NanoSSOC sun sensors. These sensors are significantly smaller than those used on the TSL bus, and cost much less, yet retain nearly the same accuracy. The small form factor and low cost provide for an important feature of the TECHBus; they allow for a configuration that provides full sky coverage for sun vector references. This is illustrated in Figure 16 where the blue cones depict the sensor's field of view. The sensors are angled such that no blind regions exist. Full sky coverage allows for simpler mission operations since constraints on the vehicle's attitude due to its sensor configuration are removed.

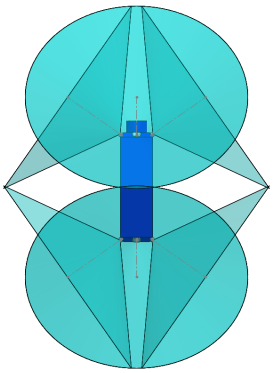

Figure 15: TECHBus full-sky sun sensor coverage.

For the most demanding accuracy missions, the TECHBus can be flown with a star tracker at the cost of payload volume. Sinclair Interplanetary's ST-16 is the most exercised and accurate small satellite star tracker available at this time. Ten units have flown since November 2013 with another 29 second generation models in production [21]. The ST-16 is manufactured for longevity in radiation environments and exceptional accuracy throughout thermal cycling. As of June 2016, Sinclair Interplanetary has reported a two times improvement in accuracy with the second generation ST-16, bringing the accuracy to <5 arc-seconds cross-boresight and <35 arc-seconds around boresight [22].

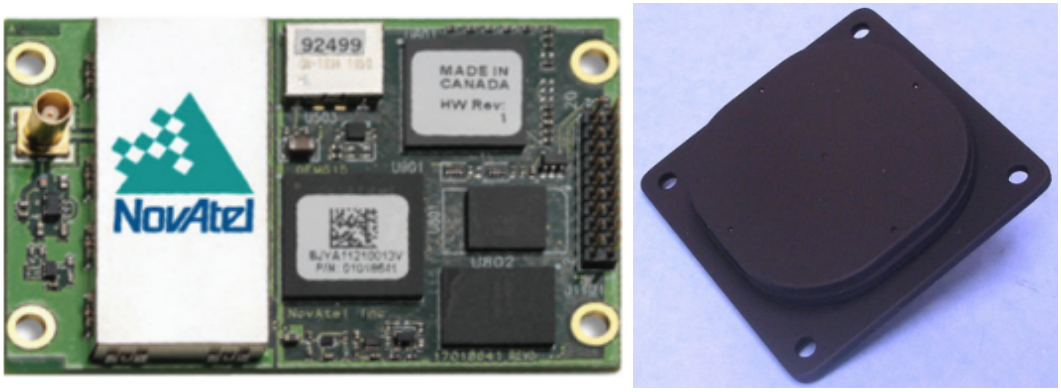

Figure 16: NovAtel OEM615 GNSS receiver (left) [26], and Antcom GPS antenna (right).

The GNSS receiver implemented on all TECHBus models by default is the NovAtel OEM615. The NovAtel has flown on several small spacecraft missions to date, and its reduced form factor from the previously used DRAGON and FOTON receivers allows for roughly 1/2U of increased payload volume over the TSL bus. The receiver uses onboard

Kalman filtering to smooth its solution. CanX-2 post-mission processing of the GNSS raw data shows position solutions down to 10 meters 3DRMS accuracy [23].

The NovAtel GNSS receiver requires an external antenna to function. The TECHBus utilizes a reliable L1/L2 antenna from Antcom. Antcom is a world leader in RF antenna solutions, and the ARMADILLO mission will fly one of its models for ionospheric sounding using GPS occultations. The high quality construction makes the antennas suitable for spaceflight, and the customization allows for RF cabling interfaces that can simplify integration in a CubeSat sized volume. For its small form factor and patch construction, the antenna offers good signal gain at zenith of 4.7 dB, and comes equipped with a 20 dB Low-Noise Amplifier (LNA).

A comprehensive summary of the TECHBus' sensors is given in Table 2 [24, 25, 21, 26, 27, 28]. Using these statistics, Section 5.2 follows with an analysis which predicts the steady state accuracy of the spacecraft's attitude determination system.

Table 2: Attitude determination sensor specifications.

Sensor	1-σ Accuracy	Units
SolarMEMS NanoSSOC Sun Sensors	0.167	deg
VectorNav VN-100 Gyroscopes	0.020	deg/s
VectorNav VN-100 Magnetometers	1.500	mGauss
Sinclair ST-16 Star Tracker	< 4 cross-BS < 35 around-BS	arc-sec
NovAtel OEM615 GNSS Receiver	10 (3DRMS)	m
Sensonor STIM300 Gyroscopes	0.004	deg/s
Honeywell HMR3200 Magnetometer	0.1	mGauss

5.2 Farrenkopf's Steady State Analysis

In 1978, Farrenkopf derived an analytical solution to the a priori and a posteriori single-axis attitude estimate error standard deviations given that the attitude was computed using an optimal estimator and has reached steady state [29]. This work has served as an important tool for ADC designers since its inception. The analytical solution provides a quick yet robust method for analyzing a system's accuracy given a set of sensors, or for directly computing the required accuracy of a mission's attitude sensors. The method is

utilized here as a verification method to show that the TECHBus' sensor suite can in fact meet typical CubeSat mission pointing knowledge requirements. Some minor modifications to Farrenkopf's original method are made to account for gyroscope integration error and are presented in Markley and Crassidis. It should be noted that while this analysis is for a single-axis estimate, several missions have reported close agreement to on-orbit performance [30].

The analysis begins with a simple problem statement: compute the a priori and a posteriori attitude estimate error standard deviations given that the vehicle: 1) integrates gyroscope measurements for measuring its dynamic motion, 2) takes an angle sensor measurement every T seconds, and 3) the gyroscope is corrupted by a zero mean white noise process and a non-constant rate bias.

The gyroscope model is defined by:

$$\dot{\theta}_{RIG} = \omega = \omega_{true} + \beta_{true} + \eta_v \tag{1}$$

where $\dot{\theta}_{RIG}$ is the rate integrated gyroscope measurement, ω is the gyroscope measurement output, β is the rate bias, and η_v is a zero mean white noise process. The rate bias is modeled as a random walk process:

$$\dot{\beta}_{true} = \eta_u \tag{2}$$

where η_u is another zero mean white noise process. The white noise processes have standard deviations σ_v and σ_u respectively. Through a number of algebraic manipulations and examining an optimal estimator's covariance matrix, the following set of equations are found as the solution to the analysis. A more thorough derivation can be found in Markley and Crassidis [30]. These equations provide attitude accuracy as a function of angle sensor update rate.

$$\sigma_\theta^- = \sigma_n \sqrt{\zeta^2 - 1} \tag{3}$$

$$\sigma_\theta^+ = \sigma_n \sqrt{1 - \zeta^{-2}} \tag{4}$$

$$\zeta = \gamma + \frac{1}{4} S_u + \frac{1}{2} \sqrt{2\gamma S_u + S_v^2 + \frac{1}{3} S_u^2} \tag{5}$$

$$\gamma = \sqrt{1 + S_e^2 + \frac{1}{4} S_v^2 + \frac{1}{48} S_u^2} \tag{6}$$

$$S_u = \frac{\sigma_u T^{3/2}}{\sigma_n},\ S_v = \frac{\sigma_v T^{1/2}}{\sigma_n},\ S_e = \frac{\sigma_e}{\sigma_n} \tag{7}$$

where σ_n is the standard deviation of the angle sensor's measurement, and σ_e is the standard deviation of the integration error for the gyroscope. Given the sensor statistics tabulated in Table 2, the Farrenkopf analysis results are shown in Figure 17. These results are combined with the control pointing error analysis into a total pointing error budget shown in Section 5.5.

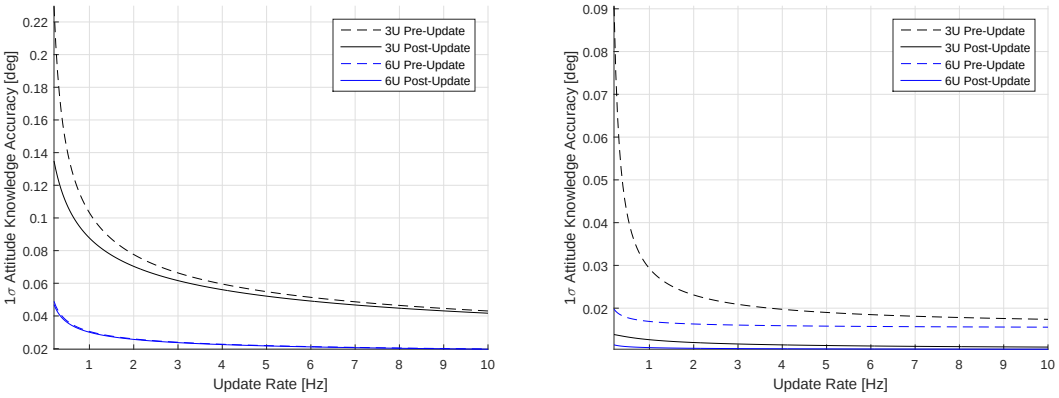

Figure 17: Sun sensor steady-state accuracy (left), star tracker steady-state accuracy (right).

5.3 Attitude Control Component Trades and Selection

The TECHBus implements two actuators in its standard configuration. Reaction wheels are utilized for primary actuation and fine pointing. Magnetic torque rods serve to provide external torques for detumbling and desaturating the reaction wheels. Cold gas thrusters developed by the LRG are optional actuators available to the TECHBus for attitude control when magnetic fields are weak or non-existent in the target orbit. The thrusters can also enable orbit maintenance and maneuver capabilities.

SSBV's CubeSat torque rods are the default magnetorquers used on the TECHBus. The same model was flown on the three TSL CubeSats, but these units have been flown on many other spacecraft and provide the simplest COTS solution. The rods are appropriately sized for 3U CubeSats, though they tend to be volumetrically inefficient when used along the vehicle's long axis. Due to the volume constraints of the TECHBus' ADC module, a

shorter rod is required. The SSDL has extensive experience designing and manufacturing torque rods. This experience was exercised for the TECHBus, and a custom Z-axis rod was designed for use. Future versions of the TECHBus will fly all in-house fabricated torque rods to save money, and serve as an educational exercise in spacecraft component design and integration. In order to make up for the increase in rotational inertia for the 6U TECHBus, pairs of SSBV torque rods were implemented on each axis. The magnetic field created by each rod adds linearly in a one-to-one manner. This fact allows for a simple solution to the 6U bus without changing system interfaces or incurring additional design costs. The nominal magnetic moment of these coils is approximately 0.2 Amp-meters squared [31].

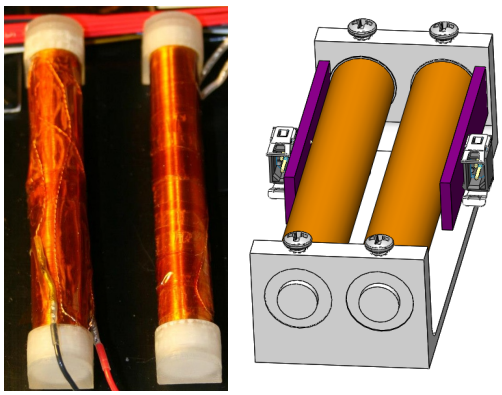

Figure 18: SSBV CubeSat magnetorquer (left), 6U TECHBus torquer pair with mount (right).

The reaction wheels utilized on the 3U and 6U TECHBus are the Sinclair Interplanetary 10 and 30 mNm-s wheels, respectively. The 10 mNm-s wheels were flown on the TSL 3U CubeSats, and nine units are currently on orbit aboard three spacecraft including the TSL's Bevo-2. The 10 and 30 mNm-s wheels share a common architecture with almost identical form factors. The 30 mNm-s wheels have 27 units on orbit aboard 11 satellites with 47 more units awaiting flight, making them the most used small spacecraft reaction wheel available. Sinclair lot screens all electronics components for radiation reliability. Furthermore, redundant motor windings and diamond coated ball bearings are implemented to prevent long-term wear out [32, 33]. Device drivers are already developed and flight qualified for the 10 mNm-s wheels, and the 30s operate with identical communication protocols. The Sinclair reaction wheels' high reliability, flight heritage, and previous LRG development

effort make them clear choices for use on the TECHBus. While new reaction wheels are appearing in the COTS market, and will be widely flown in the coming years, the Sinclair wheels provide the most reliable solution at this time.

While each reaction wheel is constructed in a reliable manner, a standard ADC subsystem nominally requires all three wheels in order to provide complete three-axis control. Many spacecraft utilize redundant reaction wheels to mitigate the risk of one failing. Unfortunately, the volume, power, and cost impact is too great for a CubeSat to carry redundant reaction wheels. However, three-axis control can be achieved with only a pair of reaction wheels if properly controlled. In order to simplify the ADC software, an already planned guidance and navigation upgrade is utilized to augment the standard control algorithms.

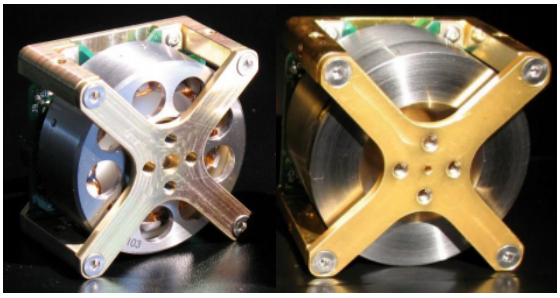

Figure 19: Sinclair Interplanetary 10 mNm-s reaction wheel (left), 30 mNm-s reaction wheel (right).

Kjellberg developed a constrained guidance and navigation system that allows for the consideration of various attitude constraints to autonomously map slew trajectories. These constraints can be keep-in/keep-out regions along sensor boresights, or angular momentum limits on actuators. Implementing this guidance system improves the reliability of the TECHBus in multiple ways. Sensor or payload integrity is guaranteed by preventing sunlight from damaging sensitive detectors, while also simplifying operations by allowing the spacecraft to autonomously determine its slew trajectories.

Figure 20 illustrates an example of the possible constraints and mapping system for Kjellberg's constrained guidance algorithm [34]. By detecting a failed reaction wheel, the constrained guidance algorithm can be set to include a zero angular momentum constraint for the failed wheel axis. The guidance algorithm will then autonomously design slew

trajectories that require no use of the failed wheel, and thus allows for a single GNC software configuration to be implemented throughout the system's operation.

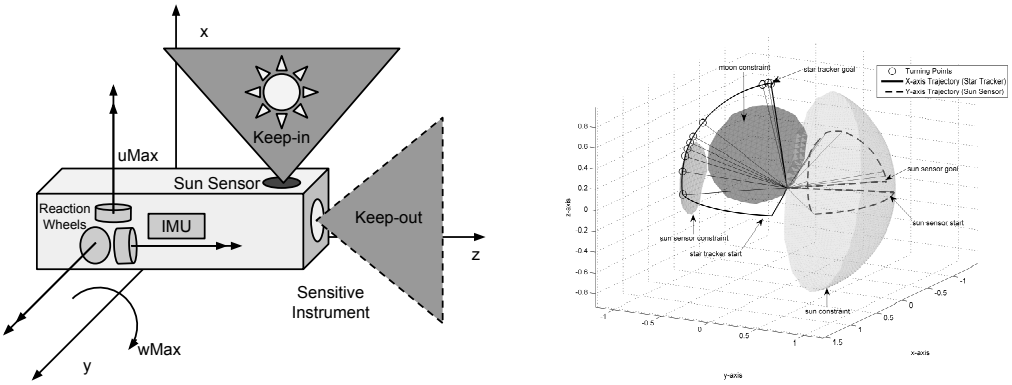

Figure 20: Kjellberg's attitude constraints and pathfinding algorithm example.

Since the ADC module of the TECHBus cannot be placed at the spacecraft's center of mass, imbalances in the wheel rotors will be amplified by the moment arm and cause a cyclic drift in the vehicle's angular momentum vector. This effect is characterized by static and dynamics imbalances. Static imbalances are caused by radial rotor mass asymmetries, and result in a periodic force applied at the location of the reaction wheels. Thus, the displacement of the reaction wheel assembly from the spacecraft center of mass results in larger disturbance torques. Dynamics imbalances arise from rotor mass variations along the rotor's spin axis which result in the rotor having a major inertia axis tilted away from the spin axis. The equations defining these effects are [35]:

$$\underline{F}_S(\omega_x, \omega_y, \omega_z) = \begin{bmatrix} S_y\omega_y^2 sin(\omega_y t + \phi_y) + S_z\omega_z^2 cos(\omega_z t + \phi_z) \\ S_z\omega_z^2 sin(\omega_z t + \phi_z) + S_x\omega_x^2 cos(\omega_x t + \phi_x) \\ S_x\omega_x^2 sin(\omega_x t + \phi_x) + S_y\omega_y^2 cos(\omega_y t + \phi_y) \end{bmatrix} \tag{8}$$

$$\underline{\tau}_S = \underline{R}_w \times \underline{F}_S(\omega_x, \omega_y, \omega_z) \tag{9}$$

$$\underline{\tau}_D = \begin{bmatrix} D_z\omega_z^2 sin(\omega_z t + \phi_z) - D_y\omega_y^2 cos(\omega_y t + \phi_y) \\ D_x\omega_x^2 sin(\omega_x t + \phi_x) - D_z\omega_z^2 cos(\omega_z t + \phi_z) \\ D_y\omega_y^2 sin(\omega_y t + \phi_y) - D_x\omega_x^2 cos(\omega_x t + \phi_x) \end{bmatrix} \tag{10}$$

where the subscript S and D represent static and dynamic respectively. ω represents the angular velocity of each reaction wheel, ϕ represents the phase angle of the sinusoidal forcing function, $\underline{R}_w$ is the location vector of the reaction wheels with respect to the spacecraft center of mass, and S and D are the static and dynamic imbalances for each wheel respectively.

The measurement of static and dynamic imbalances is dictated by ISO 1940-1 and are represented in terms of mass times distance for static, and mass times distance squared for dynamic [36]. The Sinclair Reaction wheels are balanced to ISO G1.0 in order to reduce imbalance disturbances.

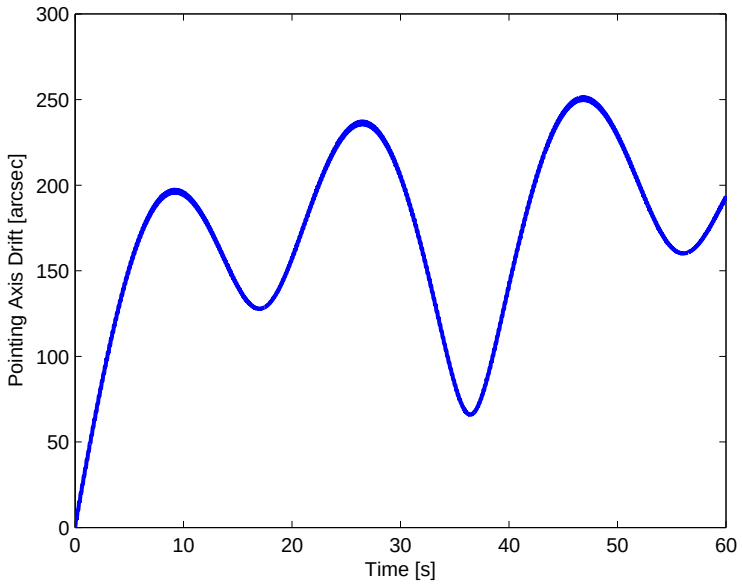

Figure 21: Pointing axis drift due to reaction wheel rotor imbalances.

A simulation was executed to analyze the perturbations these imbalances would induce upon the TECHBus' commanded pointing vector if left uncorrected. Figure 21 illustrates the simulation results. After 60 seconds, the angular drift never exceeds 250 arc-seconds, or 0.07 degrees. This is well within the stability and accuracy requirements of current advanced small spacecraft missions. Furthermore, possible mitigation strategies exist to reduce the perturbations. These include requesting tighter balancing standards, implementing imbalance disturbance prediction into the attitude control system, correcting the motion error

with accurate sensors, and maintaining low wheel angular velocities during precise pointing operations.

5.4 Control Pointing Error Analysis

The effects of control system errors must be accounted for in an ADC system's total error budget. In advanced error budgets, a variety of error sources are included such as actuator misalignment, thermal distortion, structural vibration, brushless motor oscillation, and mass property deviation. Since mass properties are generally unmeasured for CubeSats, the error induced by this effect will usually dominate. The TECHBus control error analysis only investigates mass property deviation as an error source for this reason. If more control accuracy is required, it is possible to accurately measure the CubeSat mass properties, if the resources are available.

The effect of mass property biases in a control system is characterized by a constant steady-state error. The steady-state error estimate, e_{ss}, is computed with the process used by Lee et al on the Space Interferometry Mission [37]. The error is a function of the moment of inertia error for the axis of interest, J, the percent error in the mass property estimates, $\Delta J/J$, the spacecraft's angular velocity, ω, and the controller bandwidth, BW:

$$e_{ss} = \left(\frac{\Delta J}{J}\right) \frac{(J_{max} - J_{min})}{(2\pi BW)^2} \frac{\omega^2}{J} \tag{11}$$

In the steady-state error estimate for the TECHBus, a bandwidth of 1 Hz was used with an angular rate of 5 degrees per second. A mass property error of 27% for the x and y axes, and 75% for the z axis was used for the 3U model, while errors of 12.5%, 25%, and 50% were used respectively for the 6U. The error values were determined by comparing the mass property estimates from TSL's RACE spacecraft to actual test data from the mass properties testing performed on it. In the general case, the TECHBus may not have access to mass property test facilities. The values were scaled proportionally with respect to the 6U CubeSat's mass distribution. The results of this analysis are tabulated in the combined error budget in Tables 3 and 4.

5.5 ADC System Summary

The TECHBus ADC is a three-axis reaction wheel controlled system with magnetorquers for desaturation. Redundancy is integrated throughout the system via novel guidance algorithms and backup components. The attitude determination system is equipped with a pair of IMUs and magnetometers, an array of sun sensors that provide full sky coverage, an optional star tracker for more demanding missions, and a multi-constellation GNSS receiver. The system's performance is summarized in Tables 3 and 4 with the pointing error budgets. Inputs were derived from Sections 5.2 and 5.4 for attitude determination and control respectively.

Figure 22 illustrates the the error budget in an error tree format. The first tier represents the total system error. Boxes with sub-components (e.g. Control Error and Determination Error) are the second tier. The third tier is composed of root error sources (e.g. misalignment errors, etc.). The first tier total error is found by combining the second tier in a simple sum, while the second tier components comprise the root-sum-square (RSS) of their respective third tier error sources. IMU scale factor errors are often included in these budgets, but the TECHBus IMUs come with factory calibrations that limit scale factor error to only a few hundred parts per million. At the rotation rates the CubeSat is intended to operate at, these errors fall into the noise along with thermal distortion effects, etc.

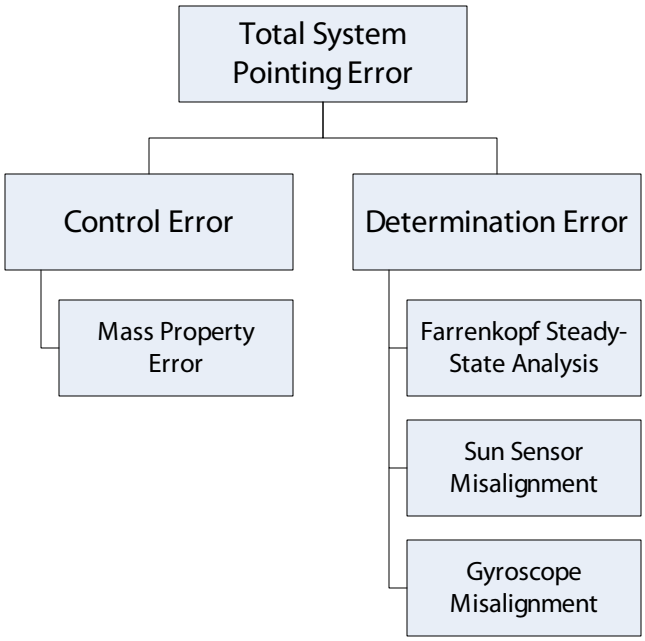

Figure 22: TECHBus pointing error budget tree.

Table 3: 3U TECHBus ADC pointing error budget.

	Error per Axis [deg]		
Error Source	X	Y	Z
Sun Sensor	0.167	0.167	0.167
Gyroscope Angular Random Walk	0.0006	0.0006	0.0006
Farrenkopf *a priori*	0.055	0.055	0.055
Farrenkopf *a posteriori*	0.052	0.052	0.052
Sun Sensor Misalignment	0.01	0.01	0.01
Gyroscope Misalignment	0.06	0.06	0.06
Attitude Determination - RSS	0.082	0.082	0.082
Attitude Controller Error	0.116	0.116	0.592
Total System Error	**0.198**	**0.198**	**0.674**
1-σ Requirement	1	1	1
Margin	**80%**	**80%**	**33%**

Table 4: 6U TECHBus ADC pointing error budget.

	Error per Axis [deg]		
Error Source	X	Y	Z
Sun Sensor	0.167	0.167	0.167
Gyroscope Angular Random Walk	0.0006	0.0006	0.0006
Farrenkopf *a priori*	0.055	0.055	0.055
Farrenkopf *a posteriori*	0.052	0.052	0.052
Sun Sensor Misalignment	0.01	0.01	0.01
Gyroscope Misalignment	0.06	0.06	0.06
Attitude Determination - RSS	0.082	0.082	0.082
Attitude Controller Error	0.018	0.023	0.147
Total System Error	**0.100**	**0.105**	**0.229**
1-σ Requirement	1	1	1
Margin	**82%**	**81%**	**69%**

Chapter 6

COMMUNICATIONS SYSTEM DESIGN

Spacecraft communications subsystems are a critical piece of any spaceflight mission. They provide the only link between the vehicle and operators or scientists back on Earth. Proper functionality of this system is imperative for the success of the mission at hand. For this reason, the TECHBus offers a communications subsystem built for performance and reliability that rivals larger spacecraft designs.

The TECHBus benefits from a variety of lessons learned from the TSL CubeSat bus development, and the RACE mission's data intensive payload. The TSL experiences led to a thorough understanding of the CubeSat radio tradespace which has allowed for subjective, and substantiated, engineering decisions that can supplement an objective analysis of COTS components. With regard to the RACE mission, its radiometer payload required a significant amount of data to be downlinked that challenged the simple amateur band UHF/VHF radio configuration.

In order to satisfy these high data throughput missions, the TECHBus implements a dedicated high data rate (HDR) radio link for science downlink. A low data rate (LDR) telecommand link will continue to use UHF frequencies for system robustness. Long wavelength signals can maintain positive link margins with omnidirectional antennas which make them reliable links even in the event of attitude control failure. To further guarantee system integrity, the telecommand link utilizes a cross-strapped radio configuration specifically enabled by the component choice explained below. Additionally, the TECHBus communications architecture allows for all science data to be transmitted via the HDR link, however the LDR link can be used as a backup.

6.1 LDR Component Trades and Selection

The LDR subsystem is charged with providing a bidirectional link between ground operators and the spacecraft for bus telemetry and commands. Highly reliable components, frequency

bands, and modulation schemes are an integral part of guaranteeing overall system integrity. A fully functioning spacecraft with no communication link to Earth is just as useless as a communicating system that cannot perform its mission.

A small number of COTS amateur band radios are currently available. Based on the experiences of the TSL CubeSat missions, a half-duplex radio was pursued to simplify the communications chain and remove failure points. The GomSpace AX-100 UHF radio module was chosen for use on the TECHBus. The unit exceeds the capabilities of the UHF/VHF full-duplex radio previously used on the TSL CubeSats. A variety of modulation schemes and data rates are supported allowing for mission variability. Furthermore, the system contains a direct GSE connection to allow for simple setting reconfiguration or debugging. One of the most important features to note is that the AX-100 has a form factor smaller than even the CDH processor. This single characteristic allows for a second unit to be integrated seamlessly without further volume cost. The two radios are integrated with the PC/104 stack in a cross-strapped manner via the GomSpace NanoDock described later in Section 8.1.

The AX-100 has been flight tested on GomSpace's GOMX-1 and GOMX-3 CubeSats, and a number of other units have flown and been delivered for use on other spacecraft. Table 5 presents the technical specifications for the AX-100 [38].

Table 5: GomSpace AX-100 radio specifications.

Parameter	Value	Units
Mass	24.5	g
Volume	65 x 40 x 6.5	mm
Voltage	3.3	V
Power Idle	0.18	W
Power TX	2.6	W
Baud Rate	1200-115200	bps
Modulation	FSK/GFSK/MSK/GMSK	-

The TSL CubeSats made use of the ISIS UHF/VHF Deployable Antenna system. The device contains four initially stowed whip antennas that are deployed into an omnidirectional dipole configuration. Additionally, the unit is designed with redundant microcontrollers that are cross-strapped to the deployment mechanism which utilizes redundant burn resistors

[39]. Because of its simplicity, highly reliable design, and extensive flight heritage, the ISIS Deployable Antenna will be used for the TECHBus. A UHF only configuration will be utilized to provide a redundant pair of telecommand antennas.

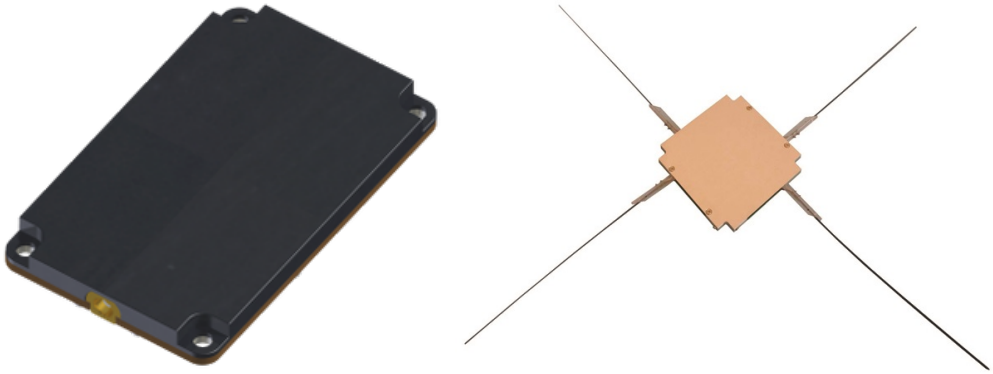

Figure 23: GomSpace AX-100 UHF radio (left), and ISIS Deployable Antenna system (right).

6.2 HDR Component Trades and Selection

The TECHBus HDR system is a dedicated radio link for science data. The link enables more efficient ground station passes by removing telecommand use and increasing the data rate. The TECHBus HDR makes use of S-band frequencies, and is capable of up to 1 megabit per second downlink speeds. The 1 Mb/s link offers the possibility to downlink over 100 times more data in the same amount of time as the LDR link. S-band offers a great increase in data rates, while requiring transmission power levels that CubeSat EPS systems can still satisfy.

Table 6: CPUT STX S-band transmitter specifications.

Parameter	Value	Units
Mass	95	g
Volume	96 x 90 x 17	mm
Voltage	5	V
Power Idle	0.6	W
Power TX	6	W
Baud Rate	1-2	Mbps
Modulation	QPSK/OQPSK	-

A small number of COTS S-band transmitters exist for CubeSats. The most widely used

device is the Cape Peninsula University of Technology's (CPUT's) STX S-band transmitter. The unit has flown on a number of small satellite missions, and will fly on CPUT's ZACUBE-2 mission in 2017. Its maiden flight was aboard the UK Space Agency's first national spacecraft, UKube-1. The STX transmitter is made to the PC/104 form factor, and utilizes an SPI interface to the flight computer. Table 6 displays a number of specifications for the CPUT STX device [40].

S-band antennas currently prove difficult to source for CubeSat applications. Due to the losses of high frequency signals, directional antennas must be used. In the case of small spacecraft, hemispherical patch antennas are good solutions to this problem. However, the majority of COTS patch S-band antennas are very large with respect to CubeSat dimensions. An extensive search of the tradespace was conducted before finding a state-of-the-art solution for a miniature S-band patch antenna.

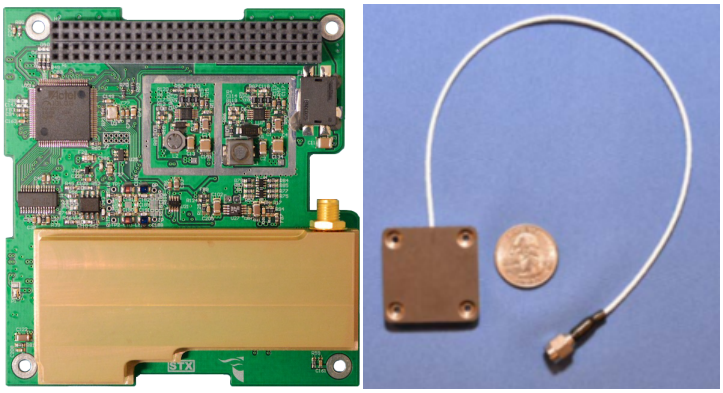

Figure 24: CPUT STX S-band transmitter (left), and Haigh-Farr CubeSat S-band path patch antenna (right).

The Haigh-Farr CubeSat S-band patch series offers a selection of tunable antennas for small spacecraft use. The square unit measures only 35 millimeters on each side and 5.3 millimeters tall, thus allowing the patch to be mounted to CubeSat exteriors without complicated structural modification. In addition to its small form factor, the Haigh-Farr antenna offers 5 dBi peak gain which is more than sufficient to close the HDR link. Table 7 shows the key specifications for the Haigh-Farr CubeSat S-band patch antenna [41].

Table 7: Haigh-Farr CubeSat S-band Patch Antenna specifications.

Parameter	Value	Units
Mass	22	g
Volume	26.25 x 26.25 x 5.3	mm
Center Freq.	2210	MHz
Polarization	RHCP	-
Pattern	Hemispherical	-
Gain (zenith)	5.0	dBi

6.3 Communications System Link Budget

A link budget is necessary for any communications system in order to fully characterize its ability to meet the system requirements. Various loss factors and gain multipliers are combined to fully define the expected received power at the receiving antenna. Equation 12 defines the simplest equation for received power. It begins by taking the RF power input to the transmitter, P_{in}, and applying an efficiency factor, η_{tx}. These two factors are then multiplied by the gain of the transmitting antenna, G_{tx}. The product of $P_{in}\eta_{tx}G_{tx}$ is referred to as the *Effective Isotropic Radiated Power*, or EIRP. Next, losses are applied to the EIRP to estimate the RF signal's power as it reaches the receiving antenna. One of the most significant losses is *path loss*, L_{path}, which is a simple function of the system frequency and distance traveled. *Atmospheric loss*, L_a, is the attenuation of the RF signal caused by the molecular composition of the atmosphere the RF signal is passing through. *Polarization loss,* L_p, is the loss due to mismatches in the transmitting and receiving antenna's polarization. The last significant loss that should always be accounted for is *pointing loss.* Pointing loss, L_θ, is a simple function of misalignment between the transmitting antenna beam's boresight, and that of the receiving antenna. The final step of a simplified link budget is to apply the receiving antenna's gain, G_{rx}.

$$P_{rec} = P_{in}\eta_{tx}G_{tx}L_{path}L_aL_pL_\theta G_{rx} \tag{12}$$

Now that the link budget process has been introduced, some other key metrics are presented. The received power of the RF signal, P_{rec}, is used to compute two critical metrics: *carrier-to-noise ratio (C/N)*, and *energy-per-bit-to-noise-density (E_b/N_0).* The two are in fact equivalent, but used indiscriminately in industry. E_b/N_0 will be used predominately

in this thesis. The E_b/N_0 of a link defines the ratio of power received per bit to the total system noise density. Communication link requirements often define a minimum E_b/N_0 that must be achieved by the system in order to guarantee a robust link. These are most often driven by the modulation/demodulation scheme implemented, as some are better at deciphering signals from noise than others. E_b/N_0 is computed by:

$$\frac{E_b}{N_0} = \frac{P_{rec}}{kT_sB} \tag{13}$$

where k is the Boltzmann constant, T_s is the system noise temperature, and B is the link bandwidth. Finally, a full system picture can be constructed for the purpose of validating a link against its requirements. A system link margin is dictated by system requirements, and represents the difference between the system E_b/N_0 and the modulation scheme's required E_b/N_0.

Comprehensive link budgets were created for both the LDR and HDR systems. The budgets were built with help from the AMSAT/IARU Annotated Link Model System. The interactive spreadsheet tool was developed by Jan King, and can be found on the AMSAT-UK website with many other useful tools [42]. The budget accounts for maximum slant ranges based on the spacecraft's orbit, computes atmospheric, ionospheric, and path losses based on frequency, and allows for input of various cabling losses. Standard antenna gain patterns are available as well as the option to input custom antenna pattern data. Furthermore, many modulation/demodulation schemes are available for selection, and drive the implementation loss factor and required E_b/N_0 thresholds. The TECHBus LDR link budget is presented in Table 8. Spacecraft inputs used in the link budget were tailored for the TECHBus system design, and utilize a standard Yagi antenna ground station design for the ground segment. An ISS-like orbit was used for range computation.

For reference, the link budget was used in reverse to approximate the maximum altitude the TECHBus could operate at without requiring a modified high-power version of the AX100. Holding all else constant, the LDR link margin becomes null at approximately 2,750 kilometers of altitude. At this same altitude, the S-band HDR link margin is still positive at just under 3 dB. While this means the TECHBus in its current form cannot complete

missions in orbits like GEO, there are viable paths forward for achieving higher transmission powers that would allow for such missions. Furthermore, the radiation environment in the 2,000-3,000 kilometer altitude range can be even more challenging than that of GEO, making it an excellent region for testing the bus' radiation mitigation approaches.

Table 8: TECHBus LDR link budget.

Parameter	Downlink Value	Uplink Value	Units
Orbit			
Altitude	400	400	km
Inclination	51.65	51.65	deg
Transmitter			
Output Power	1.0	100.0	W
in dBW	0.0	20.0	dBW
Line Losses	0.2	2.8	dB
Antenna Gain	2.2	14.4	dBi
Spacecraft EIRP	**2.0**	**31.6**	**dBW**
Path			
Pointing Loss	0.3	0.2	dB
Polarization Loss	3.0	3.0	dB
Path Loss	148.5	148.5	dB
Atmospheric Loss	4.6	4.6	dB
Ionospheric Loss	0.4	0.7	dB
Isotropic Signal @ Receiver	**-154.8**	**-125.4**	**dBW**
Receiver			
Pointing Loss	0.6	0.3	dB
Antenna Gain	18.9	2.2	dBi
Line Losses	2.0	1.7	dB
Effective Noise Temperature	1000	254	K
Figure of Merit (G/T)	-13.1	-23.6	dB/K
Signal-to-Noise Density (S/N_0)	60.0	79.4	dB-Hz
System Data Rate	9600	9600	bps
in dBHz	39.8	39.8	dB-Hz
System E_b/N_0	**20.2**	**39.6**	**dB**
Modulation Scheme	GMSK	GMSK	-
Required E_b/N_0	**8.4**	**8.4**	**dB**
System Link Margin	**11.8**	**31.2**	**dB**

The budget shows a healthy 31.2 dB link margin on the uplink side. Large margins on uplink are common due to the greater available power for transmission, and are also desired to ensure a solid link when commanding the spacecraft. Flipped bits during telecommand uplink could significantly hamper operations, or cause erratic behavior without effective error checking. The downlink budget also maintains a strong 11.8 dB margin. This indicates

Table 9: TECHBus HDR link budget.

Parameter	Downlink Value	Units
Orbit		
Altitude	400	km
Inclination	51.65	deg
Transmitter		
Output Power	6.0	W
in dBW	7.8	dBW
Line Losses	0.3	dB
Antenna Gain	5.0	dBi
Spacecraft EIRP	**12.4**	**dBW**
Path		
Pointing Loss	0.1	dB
Polarization Loss	0.0	dB
Path Loss	166.8	dB
Atmospheric Loss	4.6	dB
Ionospheric Loss	0.5	dB
Isotropic Signal @ Receiver	**-159.5**	**dBW**
Receiver		
Pointing Loss	1.2	dB
Antenna Gain	34.8	dBi
Line Losses	4.0	dB
Effective Noise Temperature	1179	K
Figure of Merit (G/T)	13.5	dB/K
Signal-to-Noise Density (S/N_0)	81.4	dB-Hz
System Data Rate	1000000	bps
in dBHz	60.0	dB-Hz
System E_b/N_0	**21.4**	**dB**
Modulation Scheme	QPSK	-
Required E_b/N_0	**9.6**	**dB**
System Link Margin	**11.8**	**dB**

that in the event of an HDR system failure, the LDR radio could potentially be reconfigured to operate at a higher data rate while still maintaining a positive link margin.

The HDR link budget is presented in Table 9. The recently installed 3 meter S-band dish at Georgia Tech was used as the ground segment for the HDR budget. The large dish offers excellent receiver gains, and will allow the GT SSDL to push the limits of COTS S-band radio transmission rates. The system achieves a 11.8 dB link margin over the QPSK required 9.6 dB. This is a healthy margin that will allow SSDL communications system researchers to increase their data rates over time.

6.4 Communications System Summary

The TECHBus communications configuration is a versatile, highly capable system with redundant telecommand radios and a dedicated high-rate mission data downlink radio. The telecommand system utilizes a pair of state-of-the-art miniaturized UHF transceivers. A deployable omnidirectional antenna is used by the telecommand link to ensure a reliable signal-to-noise ratio even in the event of attitude control failure. The telecommand system is shown to maintain positive link margins of 11.8 and 31.2 dB for downlink and uplink, respectively. The UHF half-duplex link is augmented by a high data rate S-band transmitter for science data. The S-band downlink makes use of a small patch antenna produced by Haigh-Farr, and closes its link with a margin of 11.8 dB at a 1 megabit per second data rate. The communications subsystem as a whole provides a robust, redundant, and strong link for telecommand and science data transmission between the spacecraft and ground operators.

Chapter 7

ELECTRICAL POWER SYSTEM DESIGN

The Electrical Power System of a spacecraft encompasses its power generation, storage, and distribution components. In the case of a small spacecraft, this is usually limited to solar panels, a battery charging and protection system, and a power distribution circuit. Advances in small spacecraft battery technologies have brought lithium polymer and ion cells into use. These offer significant advantages over past Nickel-metal-Hydride and Nickel-Cadmium batteries in terms of energy density and lifetime charge cycles. Lithium ion cells can be as much as four times as energy dense as Nickel-Cadmium, and twice as dense as Nickel-metal-Hydride cells [43]. Although the lithium batteries do not degrade greatly with charge cycles, they do degrade with age rather quickly. In fact, it is common for lithium battery cells to deteriorate to failure within 5 years. That said, many other battery chemistries exhibit similar behavior, and most importantly, the majority of small spacecraft missions are designed to last no longer than one or two years. This tradeoff results in greater power availability to the spacecraft throughout its mission lifetime, and major mass savings. Some caution should be given however, as lithium batteries can be dangerous to operate without appropriate safety circuitry. Care and attention must be given to properly storing and operating these systems. As with many other battery chemistries, heaters are often required to maintain safe operation if cold temperatures are expected.

Solar cells are essentially the only option available to small spacecraft in terms of power collection devices. Fuel cells are still low TRL devices, and often take up many times the volume of a CubeSat. Nuclear thermoelectric systems not only have the same volumetric limitation, but are incredibly costly and come with obvious cost and risk problems. Photovoltaic technology is slowly improving with time, and the most efficient cells available currently are Triple Junction Galium-Arsenide cells. Hundreds of thousands of these devices are currently in orbit.

A significant drawback with an EPS compared to other subsystems is that redundancy is very difficult to implement. A cross-strapped power distribution module would result in a large increase in wire harness interconnects as well as the need for complex control logic. This control logic would need to guarantee that components were powered from both power distribution boards without potentially dangerous interference. Additionally, the mass and volume cost that comes with a backup EPS is far greater than the addition of an IMU, for instance. For these reasons, the TECHBus has foregone implementing redundancy with its EPS module. To mitigate the risk, the system relies on significant flight heritage and extensive qualification testing of all EPS components.

7.1 Power Storage and Distribution Trades and Selection

The battery and power distribution system chosen for use on the TECHBus is the GomSpace P31us. The system integrates the power distribution and battery charging/protection functions into a seamless unit that simplifies the overall EPS, and ultimately uses less volume. The BP series of battery packs employs lithium ion batteries. However, it is important to note that the system uses lithium 18650 cells. These lithium ion cells are widely used throughout modern technology in laptops and other portable computing systems. While their use is limited in space flight, their wide use in terrestrial applications has established their safety and reliability. The P31us was flown on GomSpace's own GOMX-1 and GOMX-3 missions. Over 100 other units have been sold for flight since the product's introduction in 2011 [44]. To improve system quality, the P31us comprises of derated electronics components.

The 3U TECHBus makes use of the BP4 system with its 4 cells in series for a nominal operating voltage of 16.8 volts. The 6U model takes advantage of its increased volume capacity, and implements the BPX pack with 8 cells configured in a 4 series-2 parallel configuration to retain the 16.8 volt operating voltage. This consistency between the 3U and 6U TECHBus ensures an identical power distribution and management profile, thus preventing NRE costs between models. The 16.8 volt BP configurations for the 3U and 6U store a total 38.5 and 77 Watt-hours respectively [45, 46]. At the time of this thesis, that

corresponds to a 28% increase in energy storage over the next leading COTS EPS system. Finally, the P31us and BP4 were qualified for use aboard the International Space Station by GomSpace for the RACE and GOMX-2 missions. This is a significant hurdle for any spaceflight battery system, and greatly increases the availability of launch opportunities for the host spacecraft.

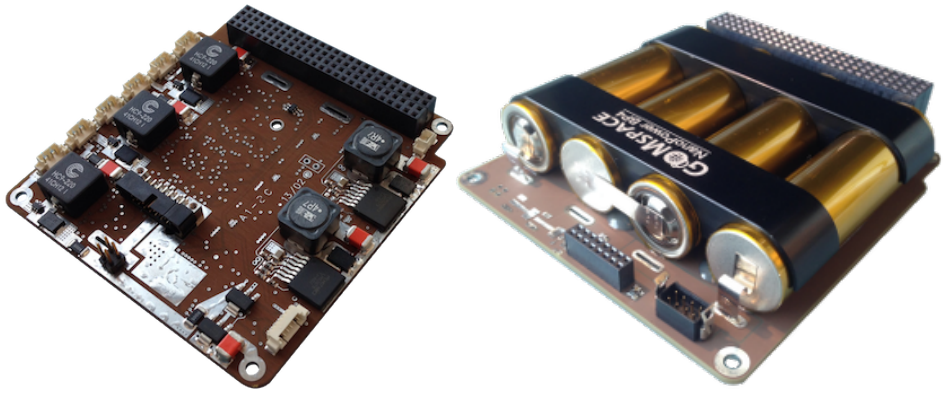

Figure 25: GomSpace P31us power distribution system (left), and BP4 battery pack (right).

The P31us' distribution module is designed with 3.3 volt, 5 volt, and raw battery voltage "always-on" output channels. An additional 6 outputs are available (3 at 3.3V, 3 at 5V) with switchable on/off states. This allows for a combination of user defined spacecraft power states. The battery charge regulators onboard the P31us are capable of receiving a total 100 Watts of input power through 3 solar panel channels. The system is configured with a series of safety cutoffs in order to protect the connected battery system. These are tied to separation switch inputs, a remove-before-flight pin, and a battery ground disconnect for various safety requirements imposed by launch vehicle demands [44]. Table 10 depicts some select parameters of the GomSpace P31us.

An important feature of the P31us to note is its direct GSE interface, similar to that of the AX100. This simple addition provides a direct terminal link to the EPS microcontroller that is routed to the spacecraft's external GSE interface. The GomShell, as it is called, can be used to debug anomalies, change parameters, and reset watchdog settings. This direct connection to the EPS firmware eliminates the need for complicated flight software development meant only for debugging the EPS, thus removing the opportunity for error

Table 10: GomSpace P31us power module specifications.

Parameter	Value	Units
Mass	100	g
Volume	90 x 90 x 20	mm
Battery Voltage	12-16.8	V
Input Voltage	0-17	V
Max Input Current	2	A
3.3V Max Output Current	5	A
5V Max Output Current	4	A
Raw Batt. Max Output Current	12	A

and potential misunderstanding of the P31us' configuration state.

With respect to radiation tolerance, the EPS is not inherently designed with radiation tolerant components. However, the integrated microprocessor interfaces with a pair of watchdog timers. These watchdogs serve to detect flight software hangs, communication system failure, and can also be used to monitor the operational state of the EPS. For example, suppose the 5 volt power distribution bus has seen a radiation event, and believes a short has occurred. In this case, the EPS protection circuitry will shut off power to the 5 volt bus even though the current draw measurement is in fact at fault. The flight computer will consequently be powered off (or detect that the 5V rail has been powered off), and consequently the EPS watchdog will not be kicked. As a result, the EPS will power cycle and clear the error caused by the radiation event.

7.2 Power Generation Trades and Selection

The TECHBus leverages the extensive history and experience of the LRG in fabricating custom solar panels. The LRG first made its own panels on the FASTRAC mission dating back to the mid-2000s. This experience was carried into the TSL's CubeSat missions. The GT SSDL also has several years of experience with in-house fabricated solar panels. The custom built solar panels for the ARMADILLO CubeSat are shown in Figure 26. The in-house production saves thousands of dollars when compared to COTS available panels that lack the custom cutouts required by many missions. Solar panels alone can often make or break a CubeSat hardware budget if COTS solutions are considered.

The LRG solar panels are constructed with a simple PCB backing, and a number of Spectrolab UTJ solar cells. The UTJs are the space industry standard for photovoltaics, and are rated for 28.3% efficiency. In the form factor used by the TECHBus, each cell provides approximately 1 Watt of beginning-of-life output power in Earth orbit. As of 2010, Spectrolab reports having delivered over 2.6 million UTJs including interplanetary missions to Mars, Jupiter, and an asteroid [47].

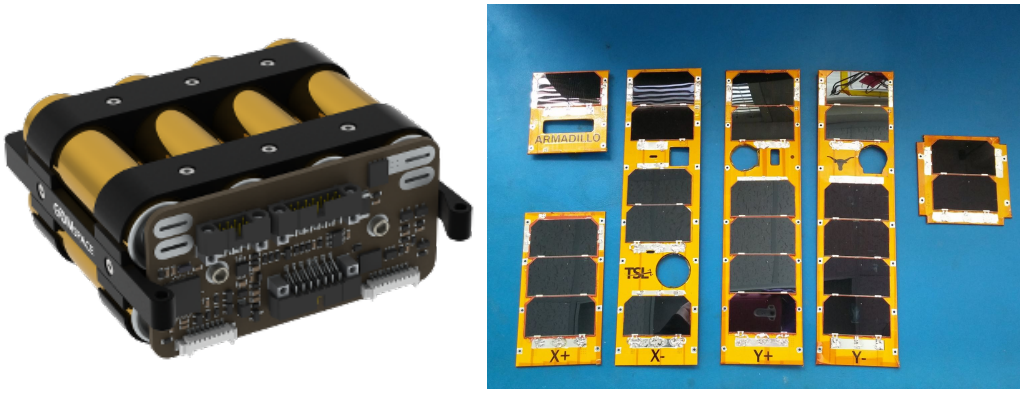

Figure 26: GomSpace BPX battery pack (left), LRG custom solar panel fabrication (right).

In addition to body mounted panels, the TECHBus is capable of utilizing deployable solar panels for missions with greater power requirements. Deployable systems are now in wide use throughout the small spacecraft industry, and the Georgia Tech SSDL is actively researching a variety of deployable structures for power collection, radio antennas, de-orbit devices, imagery calibration targets, etc [48]. This experience is being levied into the development of in-house deployable solar panels for the TECHBus, though the spacecraft bus can accommodate COTS solutions as well. The SSDL's goal is to have complete in-house deployable solar panel fabrication and flight qualification within the next few years. The tens of thousands of dollars saved in this subsystem alone will allow for more student funding and other possibilities.

7.3 Power Analysis and Budget

A critical part of any EPS design is a full system analysis in terms of current and power throughput. The EPS design must accommodate all components previously selected for use on the spacecraft or the vehicle will not function. The GomSpace P31us is capable of

delivering 5 amps on its 3.3V output bus, and 4 amps on its 5V output bus. The hardware selections for the TECHBus were compiled, and their current draw requirements rolled up into a comprehensive current budget found in Tables 11 and 12 for the 3U and 6U models respectively.

The current budgets presented demonstrate significant margins in terms of the P31us' output capabilities. The primary difference between the 3U and 6U is the increased power draw from the larger reaction wheels. The payload currents are nulled in order to provide a reference to the current throughput available to payloads that seek to use the TECHBus.

An additional analysis was performed to analyze the average power input over the course of an orbit, denoted as the power limit. The power limit values were drawn from a power analysis tool developed by Michael Herman of Professor Brian Gunter's research group at the GT SSDL. The tool combines MATLAB scripting with ephemeris and solar radiation outputs from the Satellite Toolkit (STK) software package. Depending on the mode, the average, minimum, or maximum orbit average was used. The average, minimum, and maximum values arise from seasonal changes in the orbital configuration. The analysis was performed for an ISS-like orbit with a double-deployed solar panel configuration as depicted by Figure 7. Both simulations maintained the spacecraft's attitude so as to simulate a nadir facing instrument. Tables 13 and 14 display the TECHBus power budgets at beginning of life. End of life losses for a LEO spacecraft are generally only a few percent per year, and the TECHBus baseline lifetime is 1 year. To summarize, the 3U maintains a positive margin in all modes except those that involve radio transmission. The 6U benefits from having significantly more solar cells, and maintains a positive margin in all operational modes.

Obviously, a complete system budget must include the power draw of a payload device, but the budgets shown here aide to provide requirements for payload power draw. An energy budget is often composed for operations to compute how many orbits the vehicle can maintain an operational schedule before the batteries reach a given depth of discharge. This exercise is omitted here due to the lack of payload definition.

Table 11: 3U TECHBus current budget.

	Min. Current [mA]			Max. Current [mA]			Power [W]	
	3.3 V	5 V	12-16 V	3.3 V	5V	12-16 V	Min.	Max.
1.0 CDH								
1.1 UNIBAP SOM	0	400	0	0	400	0	2.00	2.00
1.2 Carrier Board	50	50	0	50	50	0	0.42	0.42
2.0 ADC								
2.1 Actuators								
2.1.1 10 mNm-s Reaction Wheels (3)	0	66	0	0	630	0	0.33	3.15
2.1.2 SSBV Torque Rods (2)	0	80	0	0	80	0	0.40	0.40
2.1.3 Z-axis Torque Rod	0	40	0	0	40	0	0.20	0.20
2.2 Sensors								
2.2.1 VectorNav IMUs (2)	0	80	0	0	88	0	0.40	0.44
2.2.2 SolarMEMS Sun Sensors (8)	0	16	0	0	16	0	0.08	0.08
2.2.3 NovAtel OEM615 GPS	320	54	0	320	54	0	1.33	1.33
3.0 LDR Communications								
3.1 GomSpace AX100 (2)	110	0	0	1600	0	0	0.36	5.28
3.2 ISIS Deployable Antenna	8	0	0	9	0	0	0.03	0.03
4.0 HDR Communications								
4.1 ClydeSpace/CPUT STX-C	0	120	0	0	1200	0	0.60	6.00
5.0 EPS								
5.1 GomSpace P31us	0	0	13.13	0	0	17.50	0.16	0.28
6.0 Payload	0	0	0	0	0	0	0.00	0.00

	Max. Current		
Output Bus	3.3 V	5 V	12-16 V
CBE [mA]	1979	2558	1.46
Allowable [mA]	5000	4000	12000
Margin	60%	36%	100%

Table 12: 6U TECHBus current budget.

	Min. Current [mA]			Max. Current [mA]			Power [W]	
	3.3 V	5 V	12-16 V	3.3 V	5V	12-16 V	Min.	Max.
1.0 CDH								
1.1 UNIBAP SOM	0	400	0	0	400	0	2.00	2.00
1.2 Carrier Board	50	50	0	50	50	0	0.42	0.42
2.0 ADC								
2.1 Actuators								
2.1.1 30 mNm-s Reaction Wheels (3)	0	66	0	0	1080	0	0.33	5.40
2.1.2 SSBV Torque Rods (6)	0	240	0	0	240	0	1.20	1.20
2.2 Sensors								
2.2.1 Sensonor IMU	0	300	0	0	400	0	1.50	2.00
2.2.2 VectorNav IMU	0	40	0	0	44	0	0.20	0.22
2.2.3 SolarMEMS Sun Sensors (7)	0	161	0	0	161	0	0.81	0.81
2.2.4 NovAtel OEM615 GPS	320	54	0	320	54	0	1.33	1.33
2.2.5 Honeywell Magnetometer	0	0	13.5	0	0	18	0.16	0.29
3.0 LDR Communications								
3.1 GomSpace AX100 (2)	110	0	0	1600	0	0	0.36	5.28
3.2 ISIS Deployable Antenna	8	0	0	9	0	0	0.03	0.03
4.0 HDR Communications								
4.1 ClydeSpace/CPUT STX-C	0	120	0	0	1200	0	0.60	6.00
5.0 EPS								
5.1 GomSpace P31us	0	0	13.13	0	0	18	0.16	0.28
6.0 Payload	0	0	0	0	0	0	0.00	0.00

	Max. Current		
Output Bus	3.3 V	5 V	12-16 V
CBE [mA]	1979	3629	2.96
Allowable [mA]	5000	4000	12000
Margin	60%	9%	100%

Table 13: 3U TECHBus power budget.

	Power Draw [Watts]						
Mode	Safe/Low Power	Idle	Beacon-Idle	Downlink	Science	Beacon-Science	Charging
1.0 CDH							
1.1 UNIBAP SOM	2.00	2.00	2.00	2.00	2.00	2.00	2.00
1.2 Carrier Board	0.42	0.42	0.42	0.42	0.42	0.42	0.42
2.0 ADC							
2.1 Actuators							
2.1.1 10 mNm-s Reaction Wheels (3)	0	0.75	0.75	0.75	0.75	0.75	0.75
2.1.2 SSBV Torque Rods (2)	0.4	0.4	0.4	0.4	0.4	0.4	0.4
2.1.3 Z-axis Torque Rod	0.2	0.2	0.2	0.2	0.2	0.2	0.2
2.2 Sensors							
2.2.1 VectorNav IMUs (2)	0.44	0.44	0.44	0.44	0.44	0.44	0.44
2.2.2 SolarMEMS Sun Sensors (8)	0.08	0.08	0.08	0.08	0.08	0.08	0.08
2.2.3 NovAtel OEM615 GPS	0	1.33	1.33	1.33	1.33	1.33	1.33
3.0 LDR Communications							
3.1 GomSpace AX100 (2)	0.36	0.36	5.28	5.28	0.36	5.28	0.36
3.2 ISIS Deployable Antenna	0.03	0.03	0.03	0.03	0.03	0.03	0.03
4.0 HDR Communications							
4.1 ClydeSpace/CPUT STX-C	0	0	0	6.00	0	0	0
5.0 EPS							
5.1 GomSpace P31us	0.28	0.28	0.28	0.28	0.28	0.28	0.28
6.0 Payload	0	0	0	0	0	0	0
Total Power [W]	4.21	6.28	11.20	17.20	6.28	11.20	6.28
Power Limit [W]	6.5	10	10	10	10	10	19
Margin	35%	37%	-12%	-72%	37%	-12%	67%

Table 14: 6U TECHBus power budget.

	Power Draw [Watts]						
Mode	Safe/Low Power	Idle	Beacon-Idle	Downlink	Science	Beacon-Science	Charging
1.0 CDH							
1.1 UNIBAP SOM	2.00	2.00	2.00	2.00	2.00	2.00	2.00
1.2 Carrier Board	0.42	0.42	0.42	0.42	0.42	0.42	0.42
2.0 ADC							
2.1 Actuators							
2.1.1 30 mNm-s Reaction Wheels (3)	0	1.2	1.2	1.2	1.2	1.2	1.2
2.1.2 SSBV Torque Rods (6)	1.2	1.2	1.2	1.2	1.2	1.2	1.2
2.2 Sensors							
2.2.1 Sensonor IMUs (2)	2	2	2	2	2	2	2
2.2.2 VectorNav IMU	2	2	2	2	2	2	2
2.2.3 SolarMEMS Sun Sensors (7)	0.805	0.805	0.805	0.805	0.805	0.805	0.805
2.2.4 NovAtel OEM615 GPS	0.08	0.08	0.08	0.08	0.08	0.08	0.08
3.0 LDR Communications							
3.1 GomSpace AX100 (2)	0.36	0.36	5.28	5.28	0.36	5.28	0.36
3.2 ISIS Deployable Antenna	0.03	0.03	0.03	0.03	0.03	0.03	0.03
4.0 HDR Communications							
4.1 ClydeSpace/CPUT STX-C	0	0	0	6.00	0	0	0
5.0 EPS							
5.1 GomSpace P31us	0.28	0.28	0.28	0.28	0.28	0.28	0.28
6.0 Payload	0	0	0	0	0	0	0
Total Power [W]	9.17	10.37	15.29	21.29	10.37	15.29	10.37
Power Limit [W]	11	18	18	18	18	18	45
Margin	17%	42%	15%	-18%	42%	15%	77%

7.4 Electrical Power System Summary

The TECHBus utilizes one of the most flown CubeSat electrical power systems on the COTS market. The system is capable of providing 38 or 77 Watt-hours of energy storage. The system allows for onboard power state configuration, and provides the means to do additional power conditioning based on payload or spacecraft needs. The in-house developed and constructed body mounted solar panels provide significant cost reduction over commercially available assemblies. Furthermore, the spacecraft's configuration allows for 3.8 Watts on the 3U and 7.7 Watts on the 6U of payload power draw before its science operation mode becomes power negative. These values would increase given a TECHBus configuration that utilized deployable panels.

Chapter 8

INTEGRATED SYSTEM DESIGN

The TECHBus' subsystem integration approach is one of its more unique aspects. A completely custom structure is used to allow for complete freedom in the system's design. Ultimately, COTS small spacecraft structures have inherent deficiencies by forcing the subsystems to conform to a specific standard, orientation, or by simply requiring complicated secondary structures to mount components. The use of a custom structure design provides other benefits. For example, a novel use of the PC/104 stack connectors is implemented to reduce the number of wire harness interconnects, and thus interface failure points.

To begin, Figure 27 depicts the assembled 3U TECHBus architecture with most interfaces identified. A few significant components are illustrated that have not been previously defined. These include the ADC Interface Board, Sun Sensor Interface Boards, and Payload Interface Board.

8.1 System Integration Components

The following subsections explore the various components and design concepts that do not fit directly within a typical spacecraft subsystem. These integration components are intended to tie the bus together into a cohesive system through novel integration techniques.

8.1.1 ADC Interface Board

The ADC Interface Board is a simple PCB designed in-house that combines the entire ADC suite's signals into a single FlexPCB harness that can be connected to the flight computer through the PC/104 spine on the Service Stack. This simplifies ADC integration by allowing component wires to be interfaced at their final destination during ADC assembly rather than during module integration. Furthermore, a testbed flight computer can interface with the entire ADC via a single connection. The FlexPCB solution provides a simple one point

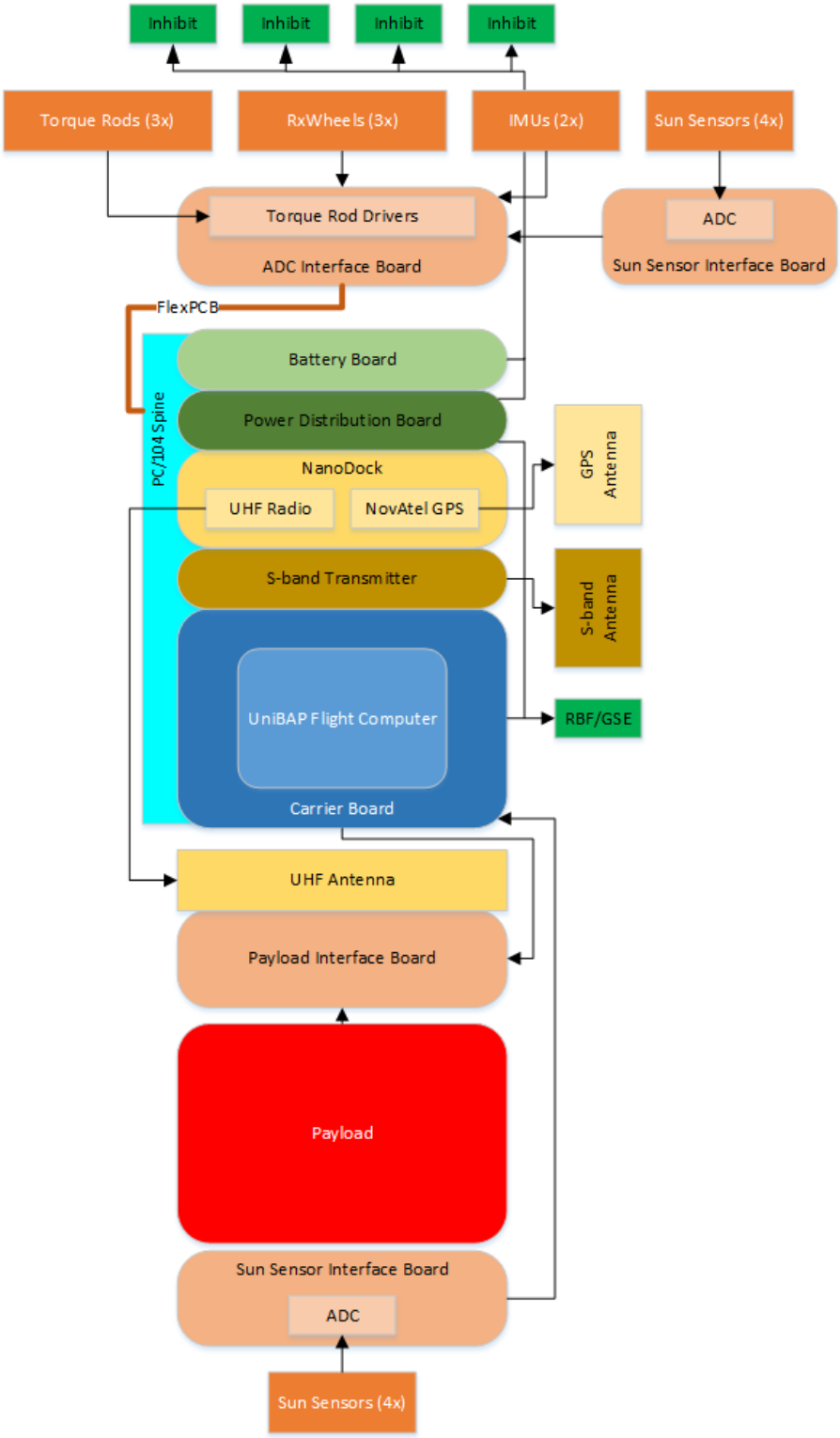

Figure 27: TECHBus Integrated Architecture diagram.

interface rather than a bundle of individually crimped wires. An example of a FlexPCB by Murrietta Circuits is shown in Figure 28, and demonstrates the use for high density inter-PCB connections. The ADC Interface Board also houses the H-bridges required to drive the magnetorquers. The same interface board is used on both the 3U and 6U system.

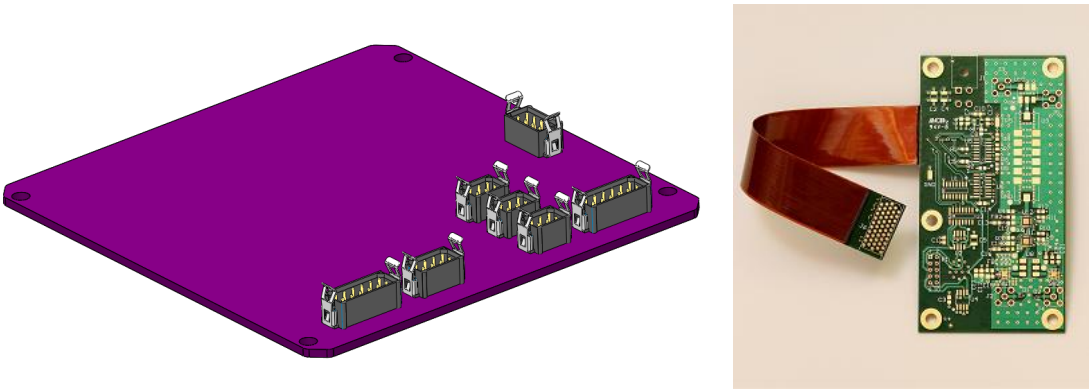

Figure 28: TECHBus ADC Interface Board (left), FlexPCB example (right).

8.1.2 Sun Sensor Interface Boards

The Sun Sensor Interface Boards only exist on the 3U TECHBus, and house an analog-to-digital converter. This converter takes the analog sun sensor outputs and converts them into a digital signal for processing by the flight computer. This processing starts with a simple conversion of the signal into a azimuth and elevation angles that correspond to the sun vector. Each set of 4 sun sensors have 8 connections that would otherwise be rerouted all the way to the flight computer. Over this long wire run, the analog signal would become corrupted by EMI. The Sun Sensor Interface Boards only require 3 SPI data lines to run to the flight computer from the entire 4 sensor set. Because the 6U has greater volume availability, the sun sensors are purchased with this analog conversion circuitry included with each device. Figure 29 (left) depicts the integrated ADC Module assembly with the top Sun Sensor Interface Board colored in purple with a circular form factor.

8.1.3 Payload Interface Board

The Payload Interface Board is a critical component that is integral in defining the TECHBus as a reusable bus. This component represents the single intentionally non-reusable part of the TECHBus by serving as the interchangeable interface to the flight computer. The Payload Interface Board acts to condition power and telemetry links from whatever the payload may require into the power and telemetry inputs and outputs of the TECHBus. For example, the TECHBus can inherently provide 3.3V, 5V, and raw battery voltage from its EPS. However, if a science instrument requires a strictly regulated 12V power input, the necessary conditioning circuitry would be designed into the Payload Interface Board. A similar concept exists for the data link in the case that the instrument utilizes a communication protocol not inherently supported by the UNIBAP flight computer.

8.1.4 System Layout

In terms of component placement on the 3U TECHBus, it has already been mentioned that the ADC was intentionally placed at the end of the bus to prevent payload interfaces from passing through the ADC Module. This idea is taken further by placing the flight computer as close to the Payload Module as possible. The ISIS UHF antenna system defines the split between the Service and Payload Modules, and houses the Payload Interface Board. Typically, the ISIS antenna can mount a small solar panel on one side. This mounting availability is utilized for the Payload Interface Board. Figure 29 (right) shows the TECHBus Service Module assembly with the Payload Interface Board colored in purple.

The 6U TECHBus makes use of the exact same Service Stack as the 3U TECHBus with the exception of the the BPX instead of the BP4 power module. This allows for identical integration and testing processes between the 3U and 6U models. To accommodate the alternative attitude control components, a different yet similar integration strategy is implemented on the 6U bus. While the 3U ADC is integrated into a self contained module, the 6U is integrated into a small set of subassemblies that can then be individually integrated into the primary structure. The ability to test the ADC is still maintained, and the majority

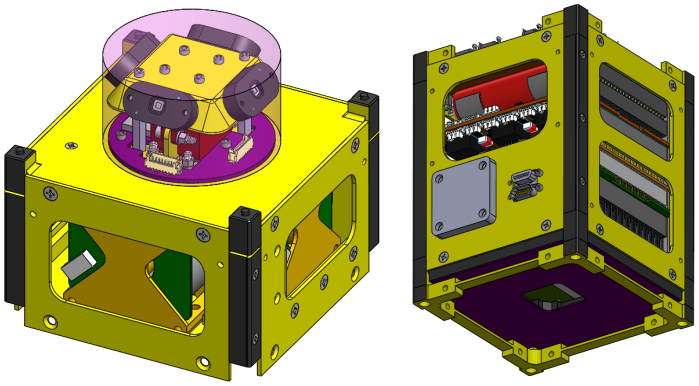

Figure 29: ADC Module (left) and TECHBus integrated Service Module (right) assemblies.

of the integration process still takes place away from the densely packed CubeSat assembly where tool access is limited. The 6U ADC subassembly can be seen in Figure 30, sits next to the Service Stack rather than above it. This places the entirety of the bus subsystems into the topmost 2U of the 6U CubeSat. The Payload Interface Board sits just below the ADC components, and the ADC Interface Board is reused from the 3U design. Finally, an EMI bulkhead separates the bus avionics from the remaining volume available to the payload. Some advanced payload instruments can be very sensitive to EMI, so the bulkhead is intended to mitigate any interference due to the bus avionics or ADC components. The 6U TECHBus layout is shown in Figure 30.

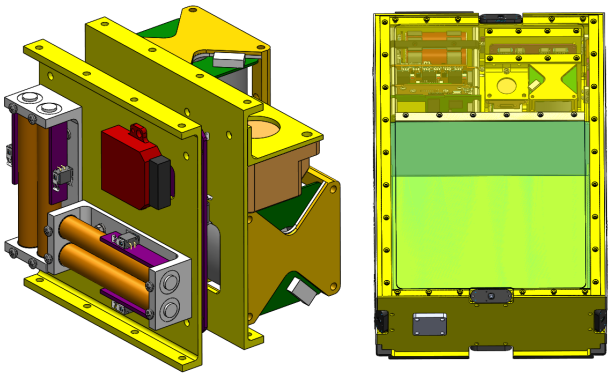

Figure 30: 6U ADC subassembly (left), and 6U TECHBus layout (right).

8.1.5 The PC/104 Spine

A large source of failure points on a spacecraft are the various wire harnesses that interconnect all of the system's components. It is simple to grasp the concept that having a single required wire is more robust than having a collection of them, unless they are redundant of course. Each wire must be crimped by a technician, installed into its connector housing appropriately, and the connector installed to its mating socket properly. If even one pin is crimped poorly an entire component could fail to function or damage other components. With this principle in mind, as well as the fact that the TECHBus is a university student-built system, effort has been placed into removing as many of these failure points as possible. One such design choice is to route signals through the PC/104 spine.

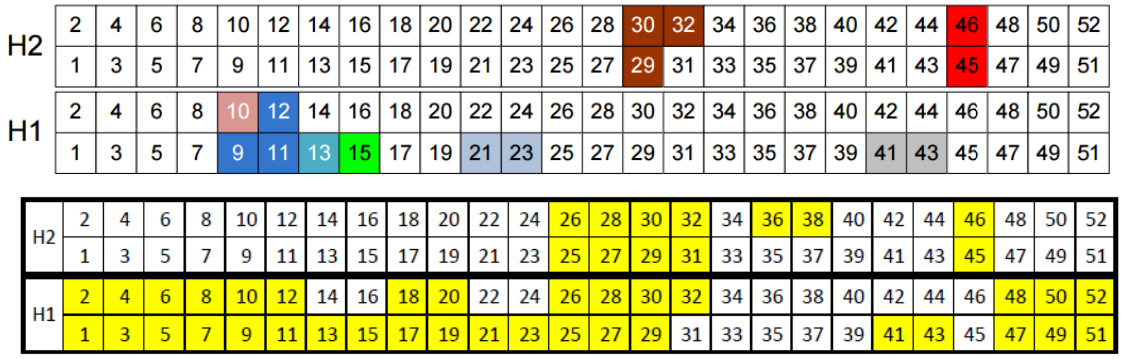

Figure 31: Standard PC/104 utilization (top), TECHBus PC/104 utilization (bottom).

The PC/104 connectors are usually under utilized by CubeSat components, and otherwise add unnecessary mass to the spacecraft. To increase the system reliability and make use of these under utilized connections, the entirety of the ADC module is connected to the PC/104 spine via the previously mentioned FlexPCB. The PC/104 spine then routes the signal directly to the flight computer interface board with the robust, solid connections offered by the PC/104 connectors. The alternative design would route some 50+ individual wires through the cramped Service Module to the interface board where several headers would be required to receive the connections. The FlexPCB design, however, reduces the excess crimp points to a single interconnect, and frees up PCB space for more useful components on the flight computer interface board. Figure 31 shows a standard PC/104 allocation

versus the pin allocation used on the TECHBus. White pins are unallocated. It is apparent that even with the entire ADC subsystem routed through the PC/104 spine there is potential for even more use.

8.1.6 GomSpace NanoDock

The final component that ties the TECHBus together is the GomSpace NanoDock. This device acts as a hub between various GomSpace components, and allows for a simple one board packaging solution that meets the PC/104 standard. The NanoDock has four individual slots for components with power and data routing to the PC/104 connector. For the TECHBus, the two AX100 radios occupy the top slots of the Dock. The Dock is also made with a special fifth port that is designed for mating the NovAtel OEM615 at the cost of the two bottom slots. This is an integral feature that simplifies the NovAtel's integration with the rest of the system. The NanoDock takes three different components, and essentially makes them into a single PC/104 board that can be gracefully integrated with the rest of the Service Stack.

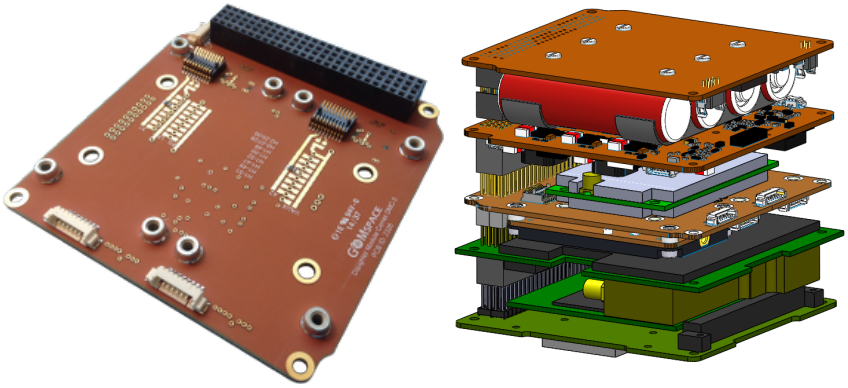

Figure 32: GomSpace NanoDock (left), TECHBus integrated Service Stack (right).

The NanoDock and integrated Service Stack are shown in Figure 32. The BP4 battery pack sits at the top of the stack, which is replaced by the BPX for the 6U with minor fastener swaps. The P31us power management board is integrated below the BP4, followed by the NanoDock. The NovAtel GNSS receiver can be seen in the center with its silver RF shielding. The CPUT S-band transmitter is mounted below the NanoDock, and finally the CDH Interface Board and UNIBAP flight computer complete the stack. To round out the

Service Module, the S-band and GPS antennas are precisely located to ensure no interference with their RF cabling and the Service Stack. Care was taken to orient the PC/104 spine orthogonal to the antenna mounting surface to allow the maximum clearance. The final integrated Service Module with antenna mounting can be found in Figure 29.

8.2 Structural Component Architecture and Design

The design of structural components for a spacecraft is often overlooked or underestimated in its complexity. However, the harsh launch environment that spacecraft must endure can present a significant challenge to structural engineers. Fortunately, due to the containerized storage and miniature nature of CubeSats, much of the vibration and g-loading is handled without extensive design or analysis. The structural design has many more responsibilities, however. It serves to unite the spacecraft subsystems into a single integral vehicle. This brings with it design challenges in terms of integration order, interface integrity, repairability, and for the TECHBus, reusability. Two important terms for the discussion of structural design are *primary structure* and *secondary structure*. Primary structure are those components that define the main parts of the vehicle's structure. They carry the majority of the load, and all subsystem components are ultimately mounted to these components. Secondary structure are the supporting brackets, etc. that aide to mount subsystem components to the primary structure. For example, the primary structure of an automobile could be considered the steel chassis to which the motor, cabin, and other components are mounted. Secondary structure of the automobile would be the various brackets that hold the battery or some other subsystem component in place.

The structural architecture of the TECHBus is derived from the TSL CubeSat bus. The modular system allows for individual subsystem integration and testing. The TECHBus implementation is revised in order to reduce cost and improve post-integration debugging or repairs. Furthermore, the components are designed with the most reusability in mind. The payload structure is the exception since it is expected to change based on the payload interface requirements for each mission. The two most significant modifications from the TSL structural architecture are breaking the monocoque structure into 2 L-shaped halves,

and reducing the exterior dimensions of the primary structure. This modification is depicted in Figure 33. The L-shaped shell halves allow for reduced manufacturing cost than the previous design. The shells can now be machined from stock L-angle at a fraction of the machine time previously required to work a complete 5 inch cube down to a hollow shell. Quotes for the TECHBus structure were requested from the same machine shop that previously fabricated the TSL CubeSat bus structure for the most direct comparison. The cost for the TECHBus' components were over 20% cheaper than those of the TSL bus.

As previously mentioned, the new architecture allows for improved repairability. For example, suppose a wire harness fails during integrated system testing. With most CubeSat structures, technicians would be required to disassemble essentially the entire spacecraft from the tubular structure so as to reach the harness. For the TECHBus, a technician can simply remove the 10-12 fasteners that retains the adjacent L-shell, remove the shell, and then have direct access to the spacecraft interior. This saves significant time, while also preventing the need to retest portions of the spacecraft that were otherwise unrelated to the failed harness.

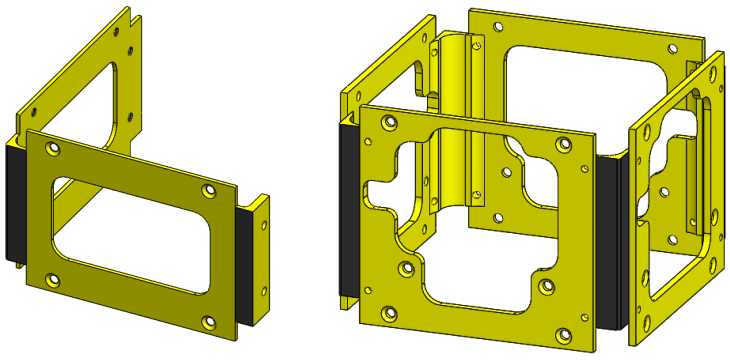

Figure 33: TECHBus half shell (left), TSL CubeSat Bus shell (right).

The exterior dimensions of the TSL CubeSat bus structure were extended from the CubeSat Standard's 100 mm in order to expand the available internal space for components. However, this consequently limited solar panel configurations to body mounted panels. By returning to the 100 mm width, several stacks of deployable solar panels can be used to increase available power while still meeting the requirements of the CubeSat Standard. A

variety of other small features make the TECHBus' primary structure robust with respect to both load paths and tolerances. As with the TSL Bus structure, the shells and section connectors are designed such that loads are not driven through fasteners in any manner. Special tabs are located on the inside walls of each L-shell to engage lateral forces into the mating shell rather than through the fasteners that connect them together. Furthermore, the section connectors and shells rest against each other along the vehicle's long axis to engage a metal-on-metal load path rather than loading the fasteners that connect them together. Tight tolerancing on these interfaces guarantee the total system tolerances can be met as defined by the various deployer standards. Finally, the hard anodizing is applied to the rail surfaces after an integrated structure polishing process is completed. This ensures a continuous rail surface even with the discontinuous structural components.

8.3 System Mass Budget

One of the most important parameters in space flight is system mass. Each kilogram takes an immense amount of energy to place into orbit. Spacecraft and launch vehicles have strict mass requirements that can drive serious design decisions. A mass budget is a method for tracking vehicle mass, and the TECHBus' mass budgets are presented in Tables 15 and 16 for the 3U and 6U respectively. The budget tracks the mass of each component on the spacecraft, as well as estimates for wiring, fastener, and conformal coating/staking mass. Contingency is placed on each component based on the value's fidelity. Components that have been physically weighed on a scale are given 2% contingency, 5% for values from datasheets, and 10% for simple estimates. Because the bus is designed without a specific payload, and is instead intended for use across many missions with various payloads, a final system margin of 3% is assigned for the 3U and 5% for the 6U. The payload mass is then back calculated from the 4 kilogram mass requirement levied by the CalPoly CubeSat Standard. A footnote on Table 15 provides the available payload mass given a 5 or 6 kilogram total mass requirement. Both bus models show sufficient payload masses to carry science instruments of the caliber currently being developed. The 4 kilogram limit on the 3U would probably limit some payloads, but fewer CubeSats are launching via P-PODs.

The P-POD is the only deployer with the 4 kilogram mass limit; the ISIPOD, NanoRacks, and Planetary Systems deployers are rated for 5, 6, and 6 kilograms respectively.

Table 15: 3U TECHBus mass budget.

		Level 2		Level 1
	CBE [g]	Contingency**	Allocated [g]	
1.0 CDH				138.0
1.1 UNIBAP SOM	25	5%	26.3	
1.2 Carrier Board	75	5%	78.8	
1.3 Payload Interface Board	30	10%	33.0	
2.0 ADC				690.6
2.1 Actuators				
2.1.1 10 mNm-s Reaction Wheels (3)	369	2%	376.4	
2.1.2 SSBV Torque Rods (2)	54	2%	55.1	
2.1.3 Z-axis Torque Rod	20	10%	22	
2.1.4 Torque Rod PCB (3)	15	10%	16.5	
2.2 Sensors				
2.2.1 VectorNav IMUs (2)	30	2%	30.6	
2.2.2 SolarMEMS Sun Sensors (8)	32	5%	33.6	
2.2.3 NovAtel OEM615 GPS	21.5	2%	21.9	
2.2.4 Antcom GPS Antenna	60	5%	63	
2.2.5 ADC Sun Sensor PCB	10	10%	11	
2.2.6 Payload Sun Sensor PCB	15	10%	16.5	
2.3 ADC Interface Board	40	10%	44	
3.0 LDR Communications				198.7
3.1 GomSpace AX100 (2)	49	2%	50.0	
3.2 ISIS Deployable Antenna	86.5	10%	95.2	
3.3 GomSpace Nanodock	51	5%	53.6	
4.0 HDR Communications				109.3
4.1 ClydeSpace/CPUT STX-C	84.5	2%	86.2	
4.2 Haigh-Farr S-band Antenna	22	5%	23.1	
5.0 EPS				925.9
5.1 GomSpace P31us	98.5	2%	100.5	
5.2 BP4 Battery Pack	262	2%	267.2	
5.3 Solar Panels (Body Mounted)	500	10%	550	
5.4 Inhibit Switches (4)	8	2%	8.16	
6.0 Structure				735.9
6.1 ADC Structure	244	5%	256.2	
6.2 Service Structure	195	5-10%	204.8	
6.3. Payload Structure	258	5-10%	274.9	
7.0 Fastener/Wiring	500	10%	550	550
8.0 Payload*	496.5	10%	551.7	551.7
			Total Mass	3900
			Mass Limit	4000
			Margin	3%

*CBE of 1374 for 5 kg limit, 2251.5 for 6 kg limit
**Contingency based on level of validity: 10% = Estimate
5% = Datasheet value
2% = Massed

Table 16: 6U TECHBus mass budget.

		Level 2		Level 1
	CBE [g]	Contingency*	Allocated [g]	
1.0 CDH				138.0
1.1 UNIBAP SOM	25	5%	26.3	
1.2 Carrier Board	75	5%	78.8	
1.3 Payload Interface Board	30	10%	33.0	
2.0 ADC				1052.6
2.1 Actuators				
2.1.1 30 mNm-s Reaction Wheels (3)	555	5%	582.8	
2.1.2 SSBV Torque Rods (6)	162	2%	165.2	
2.1.3 Torque Rod PCB (6)	30	5%	31.5	
2.2 Sensors				
2.2.1 Sensonor IMU	56	2%	57.1	
2.2.2 VectorNav IMU	15	2%	15.3	
2.2.3 SolarMEMS Sun Sensors (7)	45.5	5%	47.8	
2.2.4 NovAtel OEM615 GPS	21.5	2%	21.9	
2.2.5 Antcom GPS Antenna	60	5%	63	
2.2.6 Honeywell Magnetometer	23.5	2%	24	
2.3 ADC Interface Board	40	10%	44	
3.0 LDR Communications				200.2
3.1 GomSpace AX100 (2)	49	5%	51.5	
3.2 ISIS Deployable Antenna	86.5	10%	95.2	
3.3 GomSpace Nanodock	51	5%	53.6	
4.0 HDR Communications				109.3
4.1 ClydeSpace/CPUT STX-C	84.5	2%	86.2	
4.2 Haigh-Farr S-band Antenna	22	5%	23.1	
5.0 EPS				1753.0
5.1 GomSpace P31us	98.5	2%	100.5	
5.2 BPX Battery Expander	500	5%	525	
5.3 Solar Panels (Body Mounted)	1000	10%	1100	
5.4 Inhibit Switches (3)	15	10%	16.5	
5.5 Inhibit Interface Board	10	10%	11	
6.0 Structure				2148.3
6.1 Primary Structure	1855	5%	1947.8	
6.2 ADC Structure	191	5%	200.6	
7.0 Fastener/Wiring	750	10%	825	825
8.0 Payload	4656.33	10%	5173.7	5173.7
			Total Mass	11400
			Mass Limit	12000
			Margin	5%

*Contingency based on level of validity: 10% = Estimate
5% = Datasheet value
2% = Massed

DEVELOPMENT OF THE EVOLVED COMMON HARDWARE BUS (TECHBUS)

PART III

System Comparison and Summary

by

Parker L. Francis

Chapter 9

REUSABILITY ANALYSIS AND COMPARISON

Measuring the reusability of a common hardware bus is important in gauging its usefulness. If a reusable bus only retains its flight computer between missions, it is clearly not a reusable bus. Gamble presented a thorough quantitative method for computing a reusability metric [4]. While an experienced engineer may be able to qualitatively analyze a system's reusability, a quantitative analysis is always preferred. Much of the work presented here draws heavily from Gamble's method though some modifications have been made.

9.1 The Spacecraft Reusability Metric

To begin, a set of conditions must be established that dictate how the metric shall be interpreted. The following list defines those conditions and/or assumptions:

1. The reusability metric is based on the number of common components between any given set of missions under analysis.

2. A component is allocated to a mission provided that it is necessary and/or sufficient for meeting the requirements for that mission.

3. The reusability metric does not include a mission's payload since it will obviously differ between any given mission. However, components belonging to the spacecraft bus in support of the payload that would always be present shall be counted (e.g. the payload module's primary structure, but not payload specific secondary structure).

Gamble presented three different metrics for spacecraft reusability: hardware, software, and systems engineering processes. The method used hereafter is a modified version of the hardware metric given in her thesis. A true software analysis would take a significant amount of time to complete, and may not directly reflect the complexity or time required to reimplement a software package. The method presented below attempts to bridge the gap

between a complete software analysis, and a combined hardware and software effort required to implement a component change between missions. A weighting factor is introduced to differentiate a component swap that would only require minor hardware changes versus a component that requires major software redesign. The metric is computed as follows:

$$NR = \frac{\sum_{i=1}^{M} W_i \cdot component\_change}{\sum_{i=1}^{N} W_i \cdot component} \tag{14}$$

where NR is the non-reusable value (usually presented as a percentage), M is the total number of component changes among all compared missions, N is the total number of components among all compared missions, W_i is a weighting factor described in detail later. A *component change* is defined as a component quantity change or component swap between the compared missions. A *component* is simply an identified piece of hardware utilized within the bus design.

The weighting factor, W_i, can take on a value of 1, 3, or 5. A 1 represents a simple hardware change (bolt hole relocation, etc.) or a software variable/setting change. A 3 signifies a significant hardware change or software driver/interface rewrite. A 5 represents a major hardware modification that affects the overall bus architecture or a software overhaul. These weighting factors are obviously not scientifically resolved, but should serve the purpose of combining the important software aspect of reusability, and capturing the difference in complexity of some component changes versus others. Future work in this area could resolve these weighting factors based on statistical data accumulated through the survey of a wide range of spacecraft missions.

As an example, the reusability of the TSL CubeSat bus has been calculated using this reusability metric and the known final configurations of Bevo-2 and ARMADILLO. Gamble presented a preliminary estimate of this value in her thesis as 91%, however, the revised metric computes the TSL CubeSat bus reusability at 74.4% based on the final hardware configurations of each satellite [4]. Table 17 shows the revised calculation. A more thorough discussion of the reusability computation is presented in the next section.

9.2 TECHBus Reusability Comparison

The TECHBus reusability computation is shown in Table 18. The Bevo-2, ARMADILLO, and MicroNimbus missions are all applied to the calculation since the TECHBus is capable of completing each in terms of power, volume, and attitude control requirements. The significant components to note that fail to be reusable are solar panel PCBs, structure with payload interfaces, and the Payload Interface Board. The final TECHBus reusability value of 94.5% is a significant 20% improvement in system reusability as compared to the TSL CubeSat Bus.

Table 17: TSL CubeSat Bus reusability calculation.

	Component Weight	Bevo-2	ARMADILLO	# Component Changes	% Non-Reusable
1.0 ADC				6	21.7%
1.1 Reaction Wheels	1	3	3		
1.2 Torque Rods	1	2	3		
1.3 Gyroscopes	1	3	3		
1.4 Sun Sensors	1	2	2		
1.5 Flight Computer	5	1	1		
1.6 ADC Interface Board	3	1	1		
1.7 GPS Receiver					
1.7.1 DRAGON	3	1	0		
1.7.2 FOTON	3	0	1		
1.6 GPS Antenna(s)					
1.6.1 PCTEL	1	2	0		
1.6.2 ANTCOM	1	0	1		
2.0 CDH				2	37.5%
2.1 Flight Computer	5	1	1		
2.2 CDH Interface Board*	3	1	1		
3.0 COM				0	0.0%
3.1 UHF/VHF Radio	5	1	1		
3.2 UHF/VHF Antenna	1	1	1		
4.0 EPS				18	23.7%
4.1 Batteries	3	1	1		
4.2 Power Board	3	1	1		
4.3 Solar Cells	1	24	23		
4.4 Solar Panels (PCBs)*	1	8	9		
5.0 STR				12	40.0%
5.1 Service Shell*	1	1	1		
5.2 ADC Shell*	1	1	1		
5.3 Payload Shell*	1	1	1		
5.4 Service Structure	2	2	2		
5.5 Reaction Wheel Mount*	1	1	1		
5.6 ADC Support Structure	1	4	6		
5.6 Service Endcap	1	1	1		
5.7 Payload Endcap*	1	1	1		
				System NR %	25.6%
				Reusability %	74.4%

* Mission payload changes required deviation between otherwise common-purpose components.

Table 18: TECHBus reusability calculation.

	Component Weight	Bevo-2	ARMADILLO	MicroNimbus	# Component Changes	% Non-Reusable
1.0 ADC					0	0.0%
1.1 Reaction Wheels	1	3	3	3		
1.2 Torque Rods	1	3	3	3		
1.3 IMUs	1	2	2	2		
1.4 Sun Sensors	1	8	8	8		
1.6 ADC Interface Board	1	1	1	1		
1.7 GPS Receiver	3	1	1	1		
1.6 GPS Antenna	1	1	1	1		
2.0 CDH					3	27.3%
2.1 Flight Computer	5	1	1	1		
2.2 CDH Interface Board	3	1	1	1		
2.3 Payload Interface Board*	3	1	1	1		
3.0 COM					0	0.0%
3.1 UHF/VHF Radio	5	2	2	2		
3.2 UHF/VHF Antenna	1	1	1	1		
3.3 S-Band Radio	5	1	1	1		
3.4 S-Band Antenna	1	1	1	1		
4.0 EPS					4	2.2%
4.1 Batteries	3	1	1	1		
4.2 Power Board	3	1	1	1		
4.3 Solar Cells	1	49	49	49		
4.4 Solar Panels (PCBs)*	1	7	6	7		
5.0 STR					8	15.7%
5.1 Service Shell	1	2	2	2		
5.2 ADC Shell	1	2	2	2		
5.3 Payload Shell*	1	2	2	2		
5.4 Service Structure	1	3	3	3		
5.5 Reaction Wheel Mount	1	1	1	1		
5.6 ADC Support Structure	1	5	5	5		
5.7 ADC Endcap	1	1	1	1		
5.8 Payload Endcap*	1	1	1	1		
					System NR %	5.5%
					Reusability %	94.5%

* Mission payload changes required deviation between otherwise common-purpose components.

Chapter 10

RELIABILITY ANALYSIS AND COMPARISON

Engineering for reliability is a major part of any spacecraft mission. Many large programs dedicate entire teams of engineers, technicians, and managers to ensure that a reliable product is designed, integrated, and operated in a robust manner. Per IEEE's 762-2006 standard, reliability is defined as "the probability that a device will function without failure over a specified period or amount of usage [49]." Depending on programmatic choices, some systems will be required to operate for a nominal amount of time given a set of environmental conditions with some probability of success (e.g. 95% reliability for 10 years in a geosynchronous orbit).

There are a variety of ways to define failure which may lead to a grouping of reliability requirements that correspond to each. For instance, a mission may require 90% reliability on its high data rate radio, but 98% on its low data rate system. Commonly used terms to separate two important failure concepts are *basic reliability* and *mission reliability*. Basic reliability is the metric used for measuring reliability where failure of any kind is unacceptable. Mission reliability is more commonly used, and measures reliability where only failure that impairs the mission is unacceptable. For example, if a mission can still operate with either its low or high data rate radios, mission reliability will take this into account. Conversely, basic reliability would consider either failure independently. Important decisions and tradeoffs are made in the early design phases of any system that define the criteria for these acceptable reliability conditions. This task is often performed by defining a set of spacecraft functions required to complete the mission, and building the reliability metric around those functions. When the simple term reliability is used hereafter, mission reliability should be inferred.

10.1 The Reliability Metric

In standard analyses, component reliability is defined by an exponential or Weibull probability distribution:

$$R = e^{-\lambda t} \; or \; R = e^{-(\alpha t)^{\beta}} \tag{15}$$

where R is the probability of success (or reliability), t is the operating time, λ is the failure rate, α is the scale parameter, and β is the shape parameter. For many components, the exponential form is sufficient. However, for more complex systems that are dominated by wear out, the more general Weibull distribution is required. Occasionally, based on the unique failure profiles of components, other distributions may be utilized to better characterize system reliability [50].

When a system is composed of many other elements connected in series (much like electrical circuits), the reliability of the entire system becomes:

$$R = e^{-\sum_i^n \lambda_i t} \tag{16}$$

where λ_i is the failure rate of the i^{th} element. MIL-HDBK-217F and MIL-STD-756B provide an extensive reference for both component failure rates and the methods for compiling a reliability statistic for a given system [51, 52].

It is crucial to make clear that the reliability metric itself is not a prediction of on-orbit probability of success. The reliability calculations discussed here are useful tools as design comparators only. MIL-HDBK-217F makes this point:

> 3.3 Limitations of Reliability Predictions - This handbook provides a common basis for reliability predictions, based on analysis of the best available data at the time of issue. It is intended to make reliability prediction as good a tool as possible. However, like any tool, reliability prediction must be used intelligently, with due consideration of its limitations.
>
> Even when used in similar environments, the differences between system applications can be significant. Predicted and achieved reliability have always been closer for ground electronic systems than for avionic systems, because the environmental stresses vary less from system to system on the ground and hence the

> field conditions are in general closer to the environment under which the data was collected for the prediction model. However, failure rates are also impacted by operational scenarios, operator characteristics, maintenance practices, measurement techniques, and differences in definition of failure. Hence, a reliability prediction should never be assumed to represent the expected field reliability as measured by the user (i.e. Mean Time Between Maintenance, Mean Time Between Removals, etc.). This does not negate its value as a reliability engineering tool; note that none of the applications discussed above requires the predicted reliability to match the field measurement.

Systems engineers who do not recognize this point can incur significant budgetary costs on their program or incur additional schedule delays. Hurley and Purdy explore this topic and the philosophy behind reliability engineering in its current state for the space industry in their publication "Designing and Managing for a Reliability of Zero [53]."

The use of the exponential and Weibull distributions give rise to three important and commonly used terms that describe spacecraft failure trends. *Infant mortality* refers to the early failure of systems with a decreasing failure rate as time increases. *Wear out* is the inverse problem where failure rate increases with time and failures occur more often with system operation. The third component is simply *constant failure* where the failures are truly random, and the failure rate does not change with time. The three of these in combination construct what is often referred to as the *bathtub curve* in reliability analysis.

It is common for spacecraft programs to complete a burn in cycle with components and software in an attempt to remove the infant mortality failures from the final system. However, small spacecraft missions are commonly pressed for schedule, and have limited testing resources. This is a possible cause for the findings of Dubos, Castet, and Saleh who showed that small spacecraft have a significantly greater infant mortality rate than medium and large vehicles [54]. The authors classified spacecraft size as 50 kg or less being small, 50 to 2500 kg as medium, and greater than 2500 kg as large. Their analysis showed small spacecraft having 2.46 times as many infant mortality failures as medium spacecraft, and 1.88 times as many as large spacecraft. Large spacecraft also show a distinct wear out phase

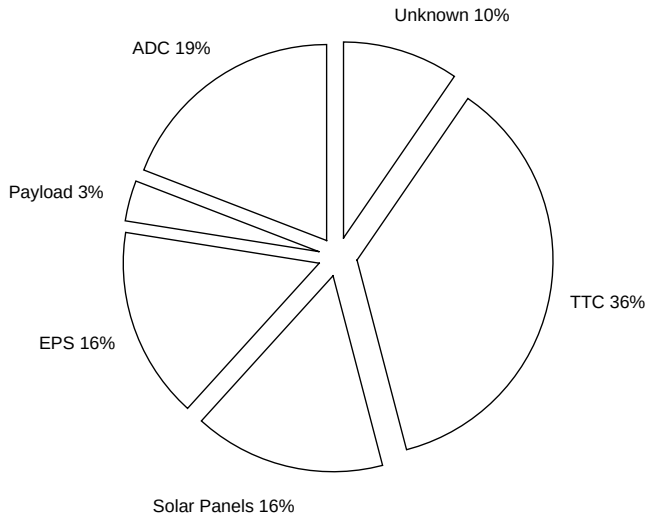

Figure 34: Subsystem contributions to spacecraft failures.

that is not as apparent in the small and medium class. In a separate publication, Castet and Saleh analyzed the failure of space vehicles by subsystem [55]. An adapted version of their results is given in Figure 34 with subsystems not applicable to the TECHBus removed. The nomenclature *TTC*, or telemetry, tracking, and command, is used in their publication, but represents the CDH and communications systems as used in this thesis. Their results were utilized during the TECHBus redundancy architecture design, and will be referred to as needed in the following subsytem descriptions.

10.2 Reliability Metrics for Redundant Architectures

When analyzing systems with redundancy, a few probability concepts and processes must be defined. The analysis process is given below as adapted from MIL-STD-756B:

1. Define the total system and its functions.
2. Define the system lifetime of interest.
3. Define the system reliability diagram.
4. Construct the mathematical reliability model.

5. Compute component reliabilities based on their sub-elements and the operating environment.

6. Compute the total system reliability using the model from step 4 and values from step 5.

As previously mentioned, defining the system and its functions is a programmatic decision that can dictate major design and quality assurance choices as the vehicle matures. Example functions could be telemetry downlink, attitude determination and control, payload power distribution, etc. The system operational lifetime is another important specification that should have been dictated in the Phase A mission definition.

A system reliability diagram like those in Figure 9 is important for a number of reasons. It aids in gaining a quick, visual intuition for the system's redundancy architecture. It also serves to help construct the system's reliability model by illustrating the interconnection or parallel paths the system can take to achieve a function's purpose.

To construct the total system reliability model, a few simple probability concepts are utilized. The basic system reliability function from which simpler expressions can be derived is:

$$R_S = P(success\ w/\ A)R_A + P(success\ w/o\ A)(1 - R_A) \tag{17}$$

where $P(success\ w/\ A)$ is the probability of system success with component A, and $P(success\ w/o\ A)$ is the probability of system success without component A. As with general probabilities, a component or system reliability cannot exceed unity. For a set of components in series with independent failure probabilities, it is found that the total probability of success is given by simply multiplying their component reliabilities:

$$R_S = R_A R_B ... \tag{18}$$

and for a pair of components in parallel, their reliabilities are added together less the probability that both operate without failure (given they are non-exclusive components):

$$R_S = R_A + R_B - R_A R_B \tag{19}$$

In more complicated systems with various series and/or parallel components or functions, equation 17 must be utilized in concert with equations 18 and 19 to construct the total system reliability model. Further examples of reliability calculations can be found in MIL-STD-756B. It should be noted that the assumptions of independent failure probabilities will likely be violated by standard spacecraft designs. However, as previously emphasized, the analysis serves as a design tool more than an actual prediction of service life.

10.3 TECHBus Reliability Comparison

The TSL CubeSat Bus and TECHBus reliability architecture diagrams are shown in Figures 35 and 36 respectively. In general, most COTS CubeSat busses offer no redundancy and are single string architectures. The TSL reliability diagram should closely resemble that of currently available COTS CubeSat busses. By simple inspection of the reliability diagrams, it is apparent how much advantage is owed to the cross-strapped architecture of the TECHBus. The only critical system functions that remain single string are the EPS and CDH systems for reasons previously discussed in the design chapters.

A detailed reliability analysis was performed for both the TSL CubeSat Bus and the TECHBus. A big picture approach was taken to approximate the number of subcomponents that belong to each substation hardware component (e.g. the number of resistors on an AX100 radio). This approach is drawn from the "Parts Count Method" explained in MIL-STD-756B's Method 2004 section [52]. A brief summary of this method is that the component is broken into a set of generic part types (e.g. resistors, capacitors, connectors, etc.), the quantity of that part type is counted, N_i, a quality level is assigned, π_i, and an environmental factor is chosen. With these four criteria, an estimated failure rate can be generated by:

$$\lambda_{item} = \sum_{i=1}^{n} N_i \lambda_G \pi_i \tag{20}$$

where n is the total number of generic parts in the component, λ_G is the generic part's base failure rate with the environmental factor applied. For brevity, the reliability calculations for the TSL CubeSat Bus and TECHBus are consolidated into Table 19. These values were calculated using a mission lifetime of 1 year, so some of the reliability values are nearly

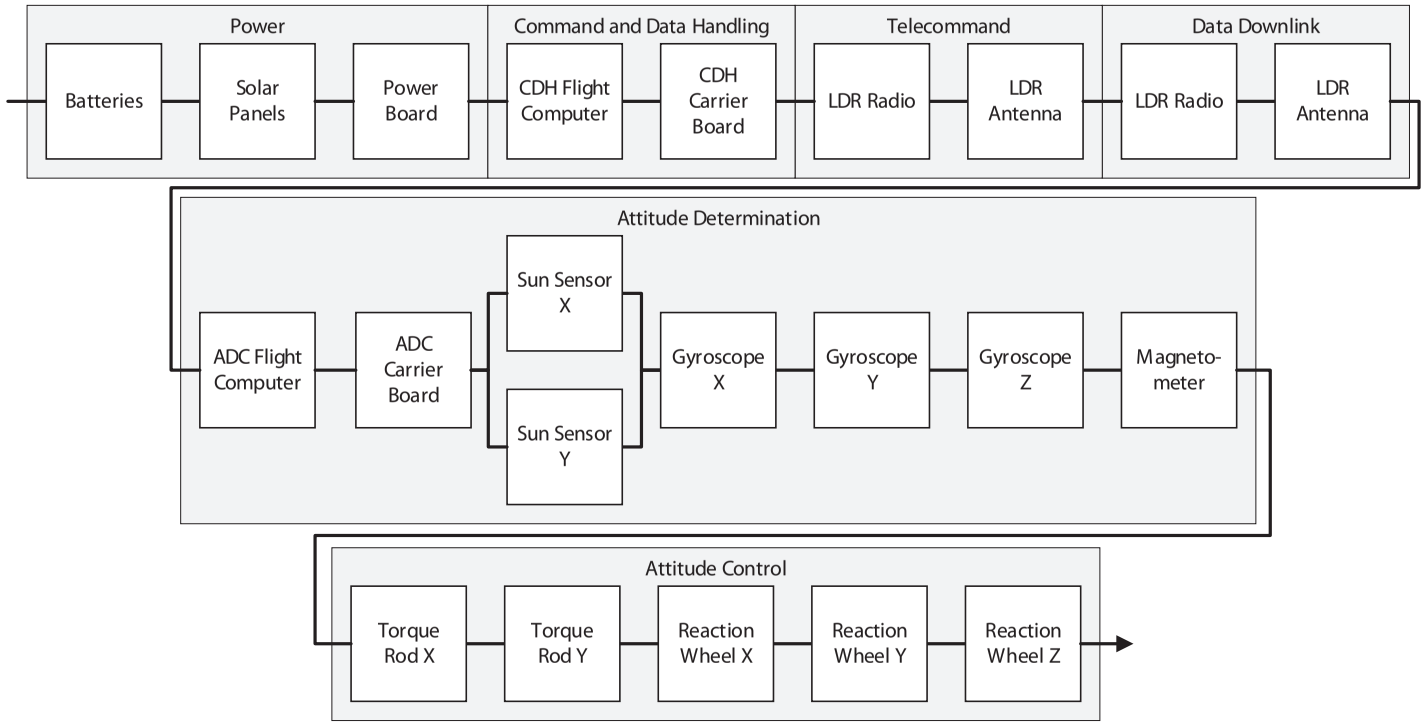

Figure 35: TSL CubeSat Bus reliability diagram.

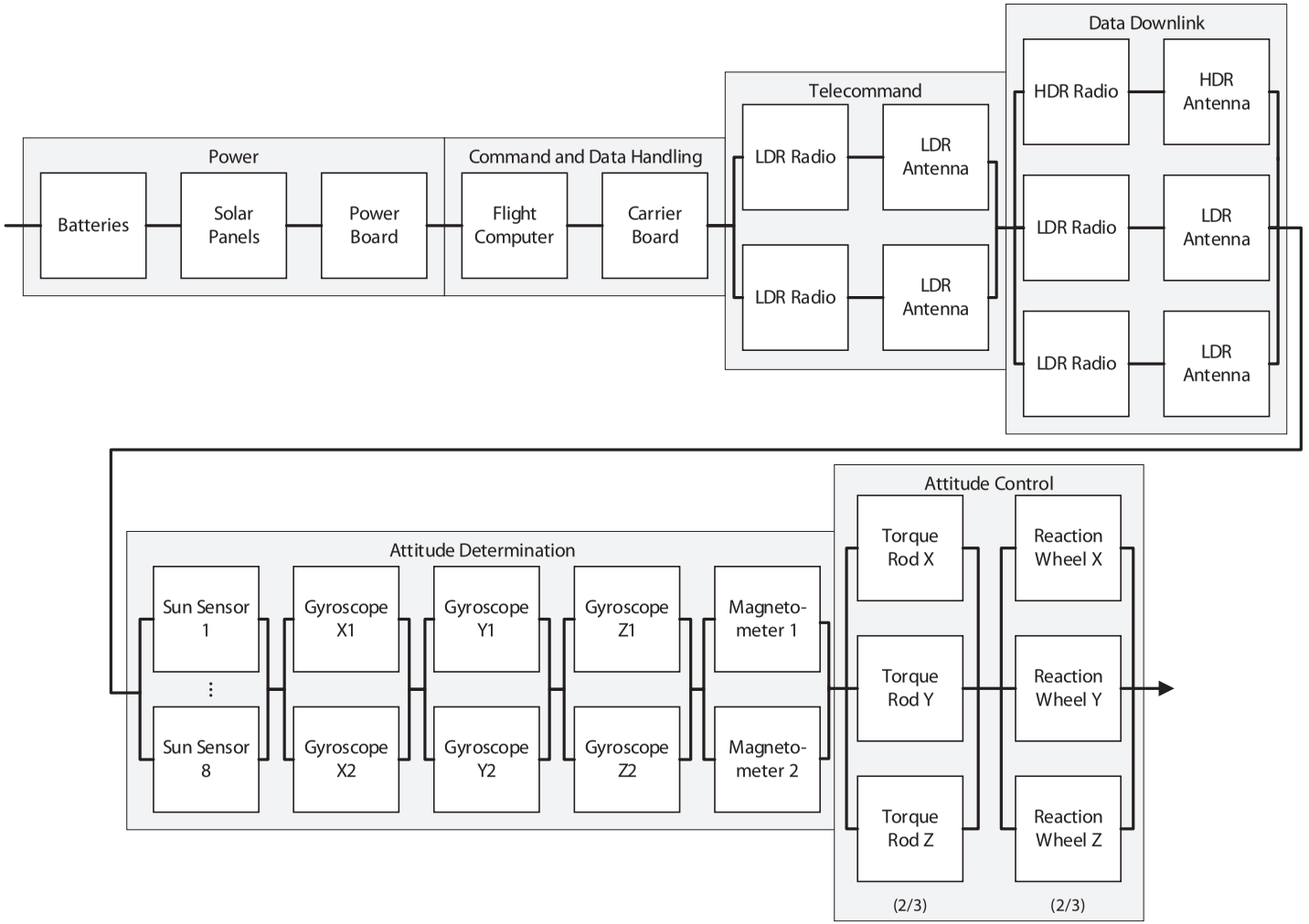

Figure 36: TECHBus reliability diagram.

unity.

Table 19: TSL CubeSat Bus and TECHBus reliability comparison.

	Reliability Value		
Spacecraft Function	TECHBus	TSL Bus	Percent Change
Electrical Power Distribution	0.99756	0.99756	0.0%
Command and Data Handling	0.98933	0.94781	4.4%
Telecommand	0.99997	0.96368	3.8%
Data Downlink	0.99999	0.96368	3.8%
Attitude Determination and Control	0.99973	0.92018	8.6%
Total	0.98662	0.80797	22.1%

The results show a major increase in system reliability on the order of 22%. As a reminder, the specific values of the reliability metrics should not hold as much weight at the relative difference between the compared systems. The reliability values are not direct representations of the expected lifetime of the vehicle, as noted in MIL-STD-756. The TECHBus sees no change between the EPS functions of itself and the TSL bus because the same configuration is utilized on both architectures. The CDH subsystem benefits from the more robust UNIBAP flight computer, and gains roughly 4% reliability. The Telecommand and Data Downlink spacecraft functions of the TSL bus were limited by the single radio configuration. However, the redundant telecommand radios greatly enhance reliability. The Data Downlink system specifically becomes almost impervious to component failures due to the triple redundant nature of that spacecraft function. As intended, the greatest improvement is seen in the ADC functions. Multiple redundant sensors are utilized throughout the system, and their benefits are seen in the 8.5% increase in reliability.

Chapter 11

PAYLOAD ANALYSIS AND COMPARISON

Beyond reusability, reliability, and cost, a significant driver for choosing a bus is the capabilities it can offer to the payload. The three following sections examine the TECHBus' volume, mass, and power available to payloads, as well as the pointing and data throughput performance.

11.1 Size, Weight, and Power

The TECHBus offers a 97x97x125 mm volume for use by payloads in the 3U model, and 106x233x215 mm volume in the 6U. These volumes come out to roughly 1.25U and 5U respectively (note, the 6U volume allowed by the PSC deployer is actually nearly 10U by strict standard). An excerpt schematic from the TECHBus Payload ICD of the 3U volume is shown in Figure 37. The small cutout features are required for structural purposes and sun sensor clearance. For comparison, some COTS bus providers market their system only requiring 1U of volume, while providing the rest of the 3U or 6U volume to the payload. However, these systems may only offer basic bus capabilities (e.g. torque rod control/stabilization, low data rate radios, no GPS, etc.).

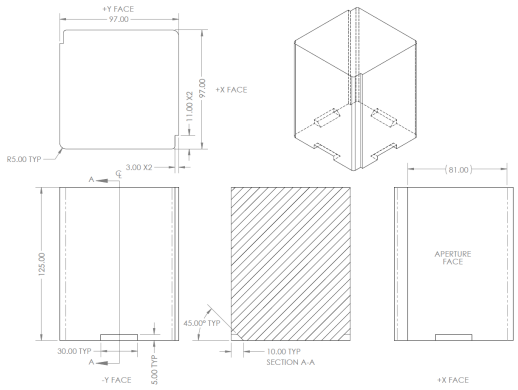

Figure 37: TECHBus 3U payload volume.

As previously mentioned in Section 8.3, the 3U TECHBus can accommodate payloads

of 0.5, 1.375, and 2.250 kilograms for a 4, 5, and 6 kilogram total mass limit respectively. The 6U TECHBus allows for a 4.7 kilogram payload out of the allowable 12 kilograms. As a reminder, these mass limits maintain a 10% contingency based on the Level 1 mass estimate for the bus. The leading COTS CubeSat busses offer 2.5 kilograms of payload mass, though the note from above should be recalled; this is likely for a baseline bus with limited capabilities.

The power availability to the payload was addressed in Section 7.4. Based on the power budget and a LEO, ISS-like orbit, the 3U TECHBus with deployables can offer 3.8 Watts of payload power before becoming power negative in the science mode. The 6U TECHBus offers 7.7 Watts with body mounted panels. Both values assume a nadir pointed payload. As mentioned in the EPS design section, deployables can be utilized to increase the power available to the payloads for operation. Another important note is that duty cycling can be introduced to the operations scheme if it is allowable to run power negative for several orbits, cease science operations, charge, and resume later. In this case, the TECHBus can offer significantly more power to the payload before being limited by the capabilities of the power distribution system.

Regulated voltages available to the payload range from 3.3 to 12 volts. Any voltages within this range can be achieved by down regulation on the Payload Interface Board, although 3.3 and 5 volt busses are available directly from the EPS. An unregulated battery voltage of 12-16 volts is also available.

Standard communication protocols available for use by payloads include: TTL/UART (all formats), I2C, SPI, CAN, and Ethernet (TCP and UDP). Protocols should be chosen based on the data rate required. For example, TTL/UART is the simplest interface, and should be chosen when flight computer interaction data rates are small. Communication busses such as SPI, CAN, and Ethernet (TCP and UDP) are more appropriate when high transfer speeds are needed. Furthermore, Ethernet TCP can provide the most robust link when packet loss is unacceptable. If a payload utilizes a communication protocol not inherently supported by the UNIBAP flight computer, the Payload Interface Board can be constructed with translation logic to adapt the protocol to one of those listed above.

11.2 Pointing Capabilities

In addition to the payload size, weight, and power offerings from a bus, its attitude control capabilities can be a mission limiting parameter. By offering the most accurate system possible, more advanced instruments can be developed and tested on small spacecraft busses. The TECHBus leverages heritage ADC algorithms, and as was shown in Section 5.5, is capable of reaching 0.2 degree and 0.1 degree accuracies for the 3U and 6U models respectively with sun sensors alone. Adding the ST-16 star tracker to the system can improve the accuracies by an order of magnitude. Commercially available CubeSat busses range in capabilities from 5-10 degrees for torque rod control and basic attitude determination, to arc-second level pointing with the use of reaction wheels and star trackers.

11.3 Data Throughput

Data throughput is becoming more relevant to small spacecraft payloads. For example, the RACE spacecraft was data limited by the TSL CubeSat Bus' UHF downlink radio. Data generation rates will increase as more advanced instruments are developed for flight on small satellites. Busses must keep up in order to remain viable platforms for advanced science missions. Section 6.4 reviews the TECHBus' communications systems. The UHF telecommand system is baselined at 9600 bits per second for link robustness, but is capable of 115,200 bits per second. However, the high data rate S-band link can transmit at up to 1 megabit per second, with research activities intending to increase that value further. Leading commercial CubeSat busses offer similar capabilities, though the majority are still operating in VHF and UHF bands with speeds no greater than 19,200 bits per second. Some X-band and Ka-band systems are becoming available in the small satellite market, but no bus is known to come configured with them by default.

Chapter 12

CONCLUSIONS

The Evolved Common Hardware Bus (TECHBus) design is a robust, reusable university small satellite bus that fits into a niche not currently filled by commercially available systems. The TECHBus' novel redundancy-implemented architecture is realized without loss of available payload size, weight, or power, making it a competitive option for researchers. The bus' design is specifically tailored toward the university engineering environment, including the use of the system as a platform for controls or software research. The common hardware approach will serve to reduce NRE cost and loss of knowledge within the university lab environment.

The TECHBus' CDH subsystem makes use of a state-of-the-art radiation tolerant FPGA system-on-a-module designed for use in safety critical environments. The single flight computer centralized architecture makes for a simple software configuration that does not require inter-computer communication schemes. Fault-tolerant command and data handling software is a future research project to be completed by the Lightsey Research Group, and will go hand in hand with the TECHBus' reliability goals. The baseline CDH software has several years of development already completed, and has been implemented on three CubeSat missions to date.

The highly capable ADC system implemented on the TECHBus offers subdegree pointing control and knowledge in its standard build, with subarc-minute pointing possible with the addition of the Sinclair Interplanetary star tracker. Redundant sensors and actuators are implemented across the spacecraft to provide a high level of robustness never seen before at the CubeSat scale. Intelligent guidance algorithms complement the hardware to provide complete control even in the event of actuator or sensor failures. The TECHBus ADC also comes with full sun sensor sky coverage, thus simplifying otherwise tedious operations planning. This capability comes at no additional cost, and in fact, is cheaper than previous

sun sensor configurations used on earlier CubeSat busses.

The communications subsystem is highly capable, and implements a fully redundant architecture to provide a reliable link with potentially several component failures. Two redundant low data rate radios make up the UHF telecommand link, and can additionally serve as backups for the high data rate S-band link. The S-band link is primarily reserved for science instrument data downlink, and offers 1 megabit per second speeds for the most demanding research instruments. The S-band radio uses a state-of-the-art miniaturized patch antenna while maintaining competitive antenna gains compared to larger systems. A redundant deployable dipole antenna is used with the telecommand system to provide stable links without the requirement of attitude stability or pointing. The deployable antenna not only offers redundant RF elements, but comes with a default dual microcontroller for robust operation throughout the mission.

The TECHBus EPS is a COTS system with the exception of in-house fabricated solar panels. The power distribution and batteries offer the industry's best in terms of power capacity, power distribution capability, and robustness. The system has flown on dozens of small satellite missions, and hundreds have been manufactured. The TECHBus' 6U model takes advantage of the battery unit's expandability, and stores 77 watt-hours while the 3U provides 38.5 watt-hours. The battery charge regulators support various deployable panel configurations, the limits of which are not exceeded even on the 6U system. In-house experience is levied to construct solar panels at a fraction of the cost of COTS systems. However, the panels make use of the best performance heritage photovoltaic cells that are commercially available.

The TECHBus' integrated system architecture brings all of the various subsystems together into a cohesive unit. Various techniques are applied to improve overall system robustness, improve integration access and repairability, and make the most efficient use of volume possible. Furthermore, special components like the Payload Interface Board act to make the TECHBus versatile and compatible with a number of different science instruments. The system is shown to be capable of flying the payloads of Bevo-2, ARMADILLO, and MicroNimbus, and is readily capable of meeting the requirements for many more.

The system is compared to other CubeSat busses that are currently available with the TSL CubeSat Bus serving as a baseline system for more in-depth comparisons. In terms of reusability, the TECHBus exceeds the capabilities of the TSL CubeSat Bus. The TECHBus is shown to be 95% reusable between the Bevo-2, ARMADILLO, and MicroNimbus missions. The final 5% is made up of payload specific interfaces that are generally intended for non-reusability in order to accommodate a variety of instruments. Furthermore, the TECHBus' architecture provides for a one year lifetime reliability of 98% compared to a single string system's 80%. These levels of reusability and reliability are unmatched on small spacecraft missions to date. On this basis alone, the TECHBus fills a void in the small spacecraft bus market where reliability and mission integrity are critical. The TECHBus is also shown to offer these novel levels of reusability and reliability without loss of payload size, mass, or power availability than comparable commercial systems.

The Georgia Tech Space Systems Development Lab will make use of the TECHBus on the upcoming MicroNimbus mission. The mission, a partnership between the Georgia Tech Research Institute and the SSDL, will be the first to demonstrate the TECHBus' capability and versatility. The TECHBus is only the beginning of a wide field of research in small spacecraft busses as the community drives their technological capabilities to that of larger vehicles. While no single satellite bus design will ever be the universal solution to every small satellite mission, the TECHBus is reduces cost and improves robustness in ways that will allow the benefits of small spacecraft to be more fully realized.

REFERENCES

[1] M. Swartwout, "The First 100 200 272 CubeSats," in *EEE Parts for Small Missions 2014 Workshop*, NASA Goddard Space Flight Center, September 2014.

[2] C. Boshuizen, J. Mason, P. Klupar, and S. Spanhake, "Results from the Planet Labs Flock Constellation," in *AIAA/USU Conference on Small Satellites*, (Logan, UT), August 2014.

[3] J. Barna, "Exponential Improvements in SmallSat Technology," in *ITU Symposium and Workshop on Small Satellite Regulation and Communication Systems*, (Prague, Czech Republic), March 2015.

[4] K. Gamble, "The Metrics of Spacecraft Design Resuability and Cost Analysis as Applied to CubeSats," Master's thesis, The University of Texas at Austin, 2012.

[5] T. Imken, "Design and Development of a Modular and Reusable CubeSat Bus," Master's thesis, The University of Texas at Austin, 2011.

[6] N. Ryan, "How does quality assurance make a difference?," tech. rep., European University Association, 2012.

[7] California Polytechnic State University, *CubeSat Design Specification*, 13th ed., February 2014.

[8] "Planetary Systems Corporation Flight Heritage." Flight Heritage Database [online database], http://www.planetarysystemscorp.com/flight-heritage [retrieved 18 January 2016].

[9] Planetary Systems Corporation, *Payload Specification for 3U, 6U, 12U, and 27U*, August 2015.

[10] C. Niederstrasser and W. Frick, "Small launch vehicles: A 2015 state of the industry survey," in *AIAA/USU Conference on Small Satellites*, (Logan, UT), August 2015.

[11] NASA Johnson Space Center, Texas A&M University, and The University of Texas at Austin, *LONESTAR Mission 2 Requirements Specification*, July 2011.

[12] NASA Office of the Chief Engineer, *NASA Space Flight Program and Project Management Requirements*, February 2010.

[13] California Polytechnic State University, *CubeSat Design Specification*, 12th ed., August 2009.

[14] L. Hansen, *Space Mission Engineering: The New SMAD*, ch. 20. Microcosm Press, 2011.

[15] Bruhnspace Advanced Projects AB, *UNIBAP Optimized Development Kit Manual*, 0.13 ed., June 2015.

[16] PHYTEC America LLC, *System on Module and Carrier Board Hardware Manual*, January 2009.

[17] 3D Plus, *Memory Module FLASH Nand 512Mx8-SOP datasheet*, August 2013.

[18] D. Sinclair and J. Dyer, "Radiation Effects and COTS Parts in SmallSats," in *AIAA/USU Conference on Small Satellites*, (Logan, UT), August 2013.

[19] 3D Plus, *Space Applications Experience and Flight Heritage Flyer*, March 2011.

[20] S. Starin and J. Eterno, *Space Mission Engineering: The New SMAD*, ch. 19. Microcosm Press, 2011.

[21] Sinclair Interplanetary, *Second Generation Star Tracker (ST-16RT) datasheet*, 2015.

[22] D. Sinclair, "Glorious First Results from ST-16RT2 Star Tracker." http://www.sinclairinterplanetary.com/news/gloriousfirstresultsfromst-16rt2startracker [retrieved July 2016].

[23] E. Kahr, O. Montenbruck, K. O'Keefe, S. Slone, J. Urbanek, L. Bradbury, and P. Fenton, "GPS Tracking on a Nanosatellite - The CanX-2 Flight Experience," in *ESA Conference on Guidance, Navigation, and Control*, (Karlovy Vary, Czech Republic), June 2011.

[24] SolarMEMS, *nanoSSOC-A60 datasheet*, 2016.

[25] VectorNav, *VN-100 IMU/AHRS datasheet*, 2016.

[26] NovAtel, *NovAtel OEM615 Receiver datasheet*, 2015.

[27] Sensonor, *STIM300 IMU datasheet*, 2015.

[28] Honeywell, *Smart Digital Magnetometer HMR2300 datasheet*, 2012.

[29] R. Farrenkopf, "Analytic Steady-State Accuracy Solutions for Two Common Spacecraft Estimators," *Journal of Guidance and Control*, vol. 1, no. 4, pp. 282–284, 1978.

[30] L. Markley, "Analytic steady-state accuracy of a spacecraft attitude estimator," tech. rep., NASA Goddard Space Flight Center, January 2000.

[31] New Space Systems, *CubeSat Magnetorquer Rod datasheet*, 2016.

[32] Sinclair Interplanetary, *10 mNm-s Reaction Wheel datasheet*, 2015.

[33] Sinclair Interplanetary, *30 mNm-s Reaction Wheel datasheet*, 2015.

[34] H. Kjellberg, *Constrained Attitude Guidance and Control for Satellites.* PhD thesis, The University of Texas at Austin, December 2014.

[35] P. Tsiotras, H. Shen, and C. Hall, "Satellite Attitude Control and Power Tracking with Energy/Momentum Wheels," *Journal of Guidance, Control, and Dynamics*, vol. 24, no. 1, pp. 23–34, 2001.

[36] International Organization for Standardization, *ISO 1940-1 - Mechanical vibration: Balance quality requirements for rotos in a constant (rigid) state*, 2nd ed., August 2003.

[37] A. Lee, J. Yu, P. Kahn, and R. Stoller, "Space Interferometry Mission Spacecraft Pointing Error Budgets," *IEEE Transactions on Aerospace and Electronic Systems*, vol. 38, no. 2, pp. 502–514, 2002.

[38] GomSpace, *NanoCom AX100 datasheet*, 2016.

[39] Innovative Solutions in Space, *Deployable Antenna System datasheet*, 2015.

[40] Cape Peninsula University of Technology, *STX S-band Transmitter datasheet*, 2016.

[41] Haigh-Farr, *Miniature Patch S-band 3755 datasheet*, 2016.

[42] J. King, "AMSAT-IARU Link Model Rev 2.5.3." http://www.amsatuk.me.uk/iaru/spreadsheet.htm.

[43] J. McDermot, J. Schneider, and S. Enger, *Space Mission Engineering: The New SMAD*, ch. 21.2. Microcosm Press, 2011.

[44] GomSpace, *NanoPower P31us datasheet*, 2016.

[45] GomSpace, *NanoPower BP4 datasheet*, 2016.

[46] GomSpace, *NanoPower BPX datasheet*, 2016.

[47] Spectrolab, *Spectrolab UTJ photovoltaic cell datasheet*, 2010.

[48] A. Long, "Trade Study and Analysis for a Deployable Drag Device for Launch Vehicle Upper Stage Deorbit," Master's thesis, Georgia Institute of Technology, 2015.

[49] IEEE Power Engineering Society, *IEEE Standard 762 - IEEE Standard Definitions for Use in Reporting Electric Generating Unit Reliability, Availability, and Productivity*, December 2006.

[50] U.S. Department of Defense, *MIL-HDBK-338B - Electronic Reliability Design Handbook*, October 1998.

[51] U.S. Department of Defense, *MIL-HDBK-217F - Reliability Prediction of Electronic Equipment*, December 1991.

[52] U.S. Department of Defense, *MIL-HDBK-756B - Reliability Modeling and Prediction*, November 1981.

[53] M. Hurley and B. Purdy, "Designing and Managing for a Reliability of Zero," in *ESA 4S Symposium*, (Funchal, Portugal), June 2010.

[54] G. Dubos and S. J. Castet, J.F., "Statistical reliability analysis of satellites by mass category: Does spacecraft size matter?," *Acta Astronautica*, vol. 67, no. 5-6, pp. 584–595, 2010.

[55] J. Castet and J. Saleh, "Satellite Reliability: Statistical Data Analysis and Modeling," in *AIAA Space Conference and Exposition*, (Pasadena, California), September 2009.